

POLITECNICO DI TORINO

Corso di Laurea Magistrale in Ingegneria Elettronica

Tesi di Laurea Magistrale

**Underwater communication
system design using
electromagnetic waves**



Relatori:

Prof. Claudio SANSOÈ

Federica LACIRIGNOLA

Candidato:

Giovanni ARRABITO

Aprile 2018

Acknowledgments

Abstract

In recent years, underwater communication has been drawing more and more attention for the large number of applications in which is needed. Specifically, the necessity of communication between divers calls for a different method than simple gestures to exchange informations and improve the quality of the communication while reducing the risks during the dives. Wireless communication has been happening through different technologies: the acoustic technology, which is the actual reference, usually employed for long-distance communication, has severe limitations because of a limited band, high latency and poor performance in shallow water, which make it unfit for diving applications; the optical technology has good performances in the short ranges, but it's strongly affected by the environmental conditions; finally, the electromagnetic waves, despite being strongly attenuated in sea water, could achieve the goal if a communication in the range of 5-10 meters is targeted. A project is currently being developed, which aims to the design of a portable computer which would allow the communication through electromagnetic waves between divers; the objective of this work was the design of the circuits for the transmission and reception that will be incorporated in the final product. The thesis is divided in three part: in the first part, a study of the physical properties of the seawater such as salinity, conductivity and permittivity has been made; then, the properties of the electromagnetic waves have been illustrated, focusing on the differences between the propagation in free space and in mediums, especially in conductive ones; following, the solutions of Maxwell equations for point sources are presented and the reasons for the choice of VLF as operational frequency is motivated. Finally, a study on the antenna will be made: first the choice of the loop antenna will be motivated; then, applying Maxwell equations, the magnetic field propagation will be described; ultimately, the antenna used for this project will be presented, showing the circuital model used for the circuit design and the measures taken on the antenna to define its parameters. In the second part an overview of the system will be shown, focusing on the components used and on the design: first the transmitter design will be addressed, explaining the principle of operation of the amplifier and the guidelines followed for the design; then, the focus will be moved on the receiver, presenting the chosen architecture for the receiving path, the design equations and the simulations made on LtSpice to check the frequency behaviour, the stability and the noise performances expected from the circuit; in the end, the circuit used for the power supply will be shown. In the third and last part, the results of the measurements on the transmitter and on the receiver will be presented. The design of the transmitter and receiver has been completed and the targeted

gain and frequency response for both the circuits have been achieved; because of lack of time, the system could not be tested in seawater, but the results obtained in the measurements made in free space are quite encouraging and suggest that the system could work fine in underwater environment. However, some optimization will be needed to achieve the final goal of the project.

Table of contents

Acknowledgments	I
1 Introduction	1
1.1 A review of underwater communication technologies	1
1.2 Objectives and organization of the thesis	2
2 Theoretical background	6
2.1 Sea water properties	6
2.1.1 Salinity	6
2.1.2 Conductivity	6
2.1.3 Permittivity	7
2.2 EM waves parameters	8
2.3 EM waves propagation	10
2.3.1 Solution of Maxwell equations for elementary sources	10
2.3.2 Attenuation and choice of VLF	12
2.3.3 Multipath propagation	13
3 Antenna and transmission	16
3.1 Antenna choice	16
3.2 Near field operation and transmission equations	17
3.3 Circuit modelling of a loop antenna	20
3.4 Measurements on the antenna	22
4 The system	26
4.1 The Arch Max development board	26
4.2 The transmitter	28
4.2.1 Class D amplifiers	28
4.2.2 Circuit design	29
4.3 The receiver	31
4.3.1 Circuit design	31
4.3.2 Sensitivity and input range of the circuit	42
4.4 The power supply	44
4.5 Final layout	47

5	System testing	50
5.1	Measurements on transmitter	50
5.2	Measurments on receiver	54
5.3	Measurements with the antennas	58
6	Conclusions and future work	64
	Bibliography	67

List of tables

1.1	Comparison of underwater wireless communication technologies [2]. . .	3
2.1	Electrical conductivity (S/m) of sea water [6]	7
2.2	EM performance underwater [2]	10

List of figures

1.1	Class C Colpitts oscillator	4
2.1	Dielectric permittivity and dielectric loss of water between 0°C and 100°C [6]	8
2.2	Attenuation of an EM wave as a function of frequency for different conductivities [8]	12
2.3	Multipath propagation in seawater [2]	13
3.1	Dipole antenna [10]	16
3.2	Circular loop antenna [11]	17
3.3	Effective magnetic permeability in ferrite rods as a function of the length-to-diameter ratio and material permeability	20
3.4	Eight lumped elements model of a magnetic antenna	22
3.5	Loop antenna as lossy inductor	22
3.6	A picture of the antenna used	23
3.7	Inductance and resistance of the antenna vs frequency	23
3.8	Inductance and quality factor of the antenna vs frequency	24
3.9	Module and phase of the antenna impedance vs frequency	24
4.1	System block diagram	27
4.2	Arch Max	28
4.3	Class D basic operation [15]	29
4.4	Class D full bridge operation [15]	30
4.5	Schematic of the power amplifier	30
4.6	Amplifier output on an inductive load	31
4.7	Schematic of the receiver	31
4.8	Frequency response of the first filter	33
4.9	Closed loop gain of the first filter	34
4.10	Frequency response of the second filter	36
4.11	Closed loop gain of the second filter	37
4.12	Closed loop gain of the third filter	38
4.13	Frequency response of the circuit	39
4.14	Output waveform with a 10kHz input	40
4.15	Output waveform with a 100kHz input	41
4.16	Output waveform with a 1kHz input	42
4.17	Output noise of the circuit	44
4.18	Schematic of TPS61032	45
4.19	Schematic of TPS63050	46
4.20	Circuit for wet contact	48

4.21	Layout of the system	48
5.1	Positive and negative terminals of the transmitting antenna	51
5.2	Detail of the wave showing the switching due to the class D amplifier	51
5.3	Differential output at the antenna terminals	52
5.4	Voltage across the antenna terminals when a 1kHz signal is applied	53
5.5	Voltage across the antenna terminals when a 100kHz signal is applied	53
5.6	Receiver output signal	54
5.7	Maximum amplitude of the receiver output signal	55
5.8	Measure of $f_{-3dB_{hi}}$	56
5.9	Measure of $f_{-3dB_{lo}}$	56
5.10	Gain measure at $f = 1kHz$	57
5.11	Gain measure at $f = 100kHz$	57
5.12	Output waveform for $V_{in,r} = 48\mu V$	58
5.13	Receiver output voltage at $d = 2.5m$	59
5.14	Receiver output voltage at $d = 3m$	60
5.15	Receiver output voltage at $d = 3.5m$	60
5.16	Receiver output voltage at $d = 10m$	61
5.17	Receiver output voltage at $d = 15m$	62

Chapter 1

Introduction

1.1 A review of underwater communication technologies

The demand for high speed wireless communication links for underwater applications has been growing in the last years. Examples of these applications are: oceanographic data collection which will require data exchange between two or more Autonomous underwater vehicles (AUVs) and other underwater sensors, underwater environmental observation for exploration and off-shore oil and gas field monitoring, coastline protection and surveillance, or, in the case of this project, communication between divers. In these regards, underwater communications have been considered exploiting three established technologies, which are: acoustics and ultrasonic signals, optical signals, and electromagnetic (EM) signals [1]. Each of these technologies has its advantages and disadvantages in their usage for underwater communications: acoustics is a proven technology and could reach really large ranges. Besides, it outperform EM waves for vertical range. However, it proves poor when transmission in shallow water is needed and it is affected by turbidity, ambient noise, salinity and pressure gradients; in addition acoustic waves can't easily cross the water/air boundary. Also, it is impossible to reach bandwidths higher than $20kb/s$ and it has a high channel latency due to the low speed of the acoustic waves; this makes acoustic waves unfit for application where high data rates and low latency is needed, such as broadband and real time underwater wireless sensor networks. On the other hand, optical communication systems, besides being low cost, can deliver high data-rates (up to Gb/s) and low latency, which are the main advantages over the acoustic technology, but at the same time they needs tight alignment of nodes and line-of-sight, and they are strongly affected by turbidity, particles and marine fouling. Besides,

it doesn't cross the water/air boundary easily. When high data-rates, low latency and immunity to ambient noise are needed, EM waves technology is probably the best choice; first of all, it could reach quite high bandwidths at close range and it has low channel latency; it is unaffected by turbidity, salinity and pressure gradients and it is immune to acoustic noise; it works in non-line-of-sight condition and it's unaffected by sediments or aeration. Finally, both acoustic and optical waves can't cross the water/air boundary, while EM waves can cross water/air and water/seabed boundaries following the path of least resistance, making the transmission much easier in shallow water and proving suitable for underwater-air communication. The worst drawback of this technology is the strong attenuation that it suffers in conductive media such as sea water, limiting the range to a few tens of meters. However, larger ranges could be reached exploiting multipath propagation [2]. Hence, EM waves technology has some advantages that are worth addressing and, since the EM signaling mechanism is different from the acoustics one, they can be seen as complementary technologies. In table 1.1 you could see a summary of the advantages and disadvantages of the techniques addressed in this section.

1.2 Objectives and organization of the thesis

The objective of the thesis is the design of a first prototype to transmit and receive signals at VLF and to use it for underwater communication. The thesis is focused on the design of the transmitter and receiver circuits and on their implementation on PCB. For what concerns the transmitter, different circuits and transmission methods have been considered; the first approach was to include the transmitting antenna in a class C Colpitts oscillator (figure 1.1, [3, 4]). In this way the generation of the signal was made in the same circuit feeding the antenna exploiting the high quality factor of the antenna itself, thus enhancing the efficiency and eliminating the need for an extra circuit for signal generation. The problem with this circuit is that, due to the high power needed for the transmission, the voltage on the capacitors and, therefore, on the transistors would have been too high, damaging the devices. The second approach was to generate square wave, exploiting the high quality factor of the antenna resonating with a series capacitor to filter out all the high frequency harmonics and leaving just the fundamental frequency desired. This

	Benefits	Limitations
RF	<ul style="list-style-type: none"> • Crosses air/water/seabed boundaries easily • Prefers shallow water • Unaffected by turbidity, salinity, and pressure gradients • Works in non-line-of-sight; unaffected by sediments and aeration • Immune to acoustic noise • High bandwidths (up to 100 Mb/s) at very close range 	<ul style="list-style-type: none"> • Susceptible to EMI • Limited range through water
Acoustic	<ul style="list-style-type: none"> • Proven technology • Range: up to 20 km 	<ul style="list-style-type: none"> • Strong reflections and attenuation when transmitting through water/air boundary • Poor performance in shallow water • Adversely affected by turbidity, ambient noise, salinity, and pressure gradients • Limited bandwidth (0 b/s to 20 kb/s) • Impact on marine life
Optical	<ul style="list-style-type: none"> • Ultra-high bandwidth: gigabits per second • Low cost 	<ul style="list-style-type: none"> • Does not cross water/air boundary easily • Susceptible to turbidity, particles, and marine fouling • Needs line-of-sight • Requires tight alignment of nodes • Very short range

Table 1.1: Comparison of underwater wireless communication technologies [2].

way the generation of the signal would have resulted way easier than generating a sine wave, but the spectral purity of the signal would have been compromised. Therefore, in the end, a signal generator implemented on a development board was used, amplified by a class D amplifier and sent to the resonating antenna. For what concerns the receiver, the circuit implemented consists in some filtering stages to cut the noise band and a low noise amplifier. The objective was to get a sensitivity

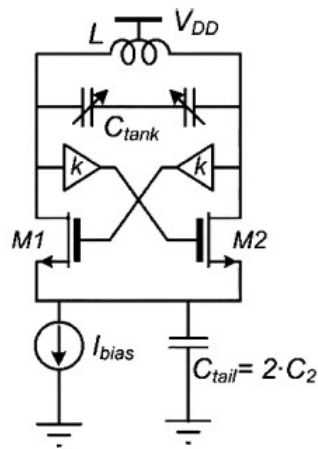


Figure 1.1: Class C Colpitts oscillator

in the order of tens of μV . The thesis is organized as follows:

- In chapter 2 some of the basic properties of sea water and of electromagnetic waves are analysed.
- In chapter 3 the choice of the antenna is addressed, and the transmission equations and circuit modelling of the antenna are described.
- In chapter 4 the design of the system is shown, focusing in detail on the different stages for the transmission and the reception and for the power supply.
- In chapter 5 the results of the testing of the circuit are shown.
- In chapter 6 some conclusions and suggestions for future works are presented.

Chapter 2

Theoretical background

2.1 Sea water properties

The main goal of this thesis is the design of a wireless system which is going to work in sea water. For this reason, the most important physical properties of this medium are briefly examined.

2.1.1 Salinity

The average salinity of the world sea waters is around 3.47%. Salinity affects EM propagation because it leads to a much severe attenuation if compared to the one in free air. This is due to a variation on the permittivity of the water, which is linked to the strength of the dipole moment of the molecules, and on the conductivity, due to the addition of ionized molecules in the water, whose molecules are not naturally polarized (low conductivity). In [5] different models have been analysed to link the salinity to water permittivity, such as the Debye model, the Stogryn model or the Klein and Swift model; it has been shown that there is a slight decrease in the permittivity of water as the salinity increase, while the so called dielectric loss slightly increases. The conductivity, instead is strictly linked to the salinity.

2.1.2 Conductivity

The conductivity of water is dependent on the concentration of dissolved salts and other chemical species in it, which tend to ionize the solution. Water itself is not a conductive medium, being its molecules not polarized, so the purer the water, the lower the conductivity (higher resistivity) will be. Also, conductivity is dependant on the temperature. In table 2.1 some values of conductivity in relation to salinity and temperature are shown.

Temperature (°C)	Salinity(g/Kg)		
	20	30	40
0	1.745	2.523	3.285
5	2.015	2.909	3.778
10	2.300	3.313	4.297
15	2.595	3.735	4.837
20	2.901	4.171	5.397
25	3.217	4.621	5.974

Table 2.1: Electrical conductivity (S/m) of sea water [6]

2.1.3 Permittivity

Permittivity in a medium is described by a complex number:

$$\varepsilon_{water} = \varepsilon_0 \varepsilon_r - j \frac{\sigma}{\omega} \quad (2.1)$$

In which:

ε_r is the relative permittivity;

$\varepsilon_0 = 8.85 \cdot 10^{-12}$ is the vacuum permittivity;

σ is the conductivity of the medium;

$\omega = 2\pi f$ is the angular frequency.

The relative permittivity itself could vary depending on different factors: salinity, temperature, frequency [5]. The variation of this parameter could be described by different models (Cole-Cole, Debye). Anyway, when working at low frequency, its value could be considered almost constant with frequency and equal to around 81 at 20°C. In figure 2.1 it is shown the variation of the relative permittivity and of the dielectric losses with temperature and frequency. The arrows show the effect of increasing temperature on the relative permittivity and dielectric loss. As you can see, for a range of frequencies up to some GHz, the relative permittivity is almost constant [6].

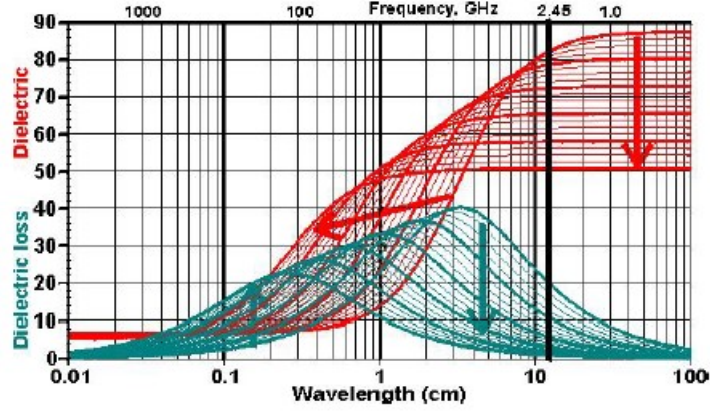


Figure 2.1: Dielectric permittivity and dielectric loss of water between 0°C and 100°C [6]

2.2 EM waves parameters

In this section some of the most important parameters of the electromagnetic waves in free space and in a medium will be examined. In free space the conductivity σ is equal to 0 and the relative permittivity is constant and equal to 1. So, in free space:

$$\begin{aligned}
 c &= \lambda_0 f; \\
 k &= k_0 = \frac{2\pi f}{c} = \frac{2\pi}{\lambda_0}; \\
 \gamma &= \sqrt{(j\omega\epsilon)(j\omega\mu)} = j\omega\sqrt{\epsilon\mu} = jk_0; \\
 \eta &= \sqrt{\frac{\mu}{\epsilon}} = Z_0 = 120\pi
 \end{aligned} \tag{2.2}$$

In which:

f is the frequency of the EM wave;

$c \simeq 300000km/s$ is the speed of the light in vacuum;

λ_0 is the wavelength of the wave in vacuum;

k_0 is the phase constant of the wave in vacuum;

γ is the propagation constant of the wave;

μ is the magnetic permeability of the medium;

η is the intrinsic impedance of the wave; Z_0 is the intrinsic impedance in free space.

When the wave is propagating in a medium, the permittivity is described by equation 2.1; depending on the relation between frequency of the propagating wave, conductivity and relative permittivity of the medium itself, there are two borderline cases: if $\frac{\sigma}{\omega} \gg \epsilon_0 \epsilon_r$ then the medium could be referred as a “conductive medium”. If, instead, $\frac{\sigma}{\omega} \ll \epsilon_0 \epsilon_r$ then the medium could be referred as a "dielectric medium" [3]. Considering now the propagation constant as described in equation 2.2 and the permittivity of a medium as described in 2.1, then:

$\gamma \simeq k_0$ in a dielectric medium;
 $\gamma \simeq \sqrt{j\omega\mu\sigma}$ in a conductive medium.

Since we're going to work in sea water, which is a good conductive medium, then we're going to work in the second condition. This leads to different parameters of the wave:

$$\begin{aligned} v &= \frac{c}{\sqrt{\epsilon_r}} < c; \\ \lambda &= \frac{v}{f} < \lambda_0; \\ \eta &\simeq \sqrt{\frac{j\omega\mu}{\sigma}} \end{aligned} \quad (2.3)$$

Working in a conductive medium greatly affects the propagation of the electromagnetic waves, because of the change in the propagation constant, as it will be described in section 2.3. An important parameter to evaluate the attenuation of a wave in a conductive medium is the so called skin depth [2]. The skin depth is a way of evaluating the effect of the skin effect, which is defined as the tendency of the AC current to distribute in a conductor such that the current density is larger near the surface of the conductor and decreases with greater depth in the conductor. The skin depth is defined as the depth in the conductor in which the current density decreases at a value of $\frac{1}{e}$ of the current density on the surface. The skin depth is given by:

$$\delta_{skin} = \sqrt{\frac{2}{\omega\mu\sigma}} \sqrt{\sqrt{1 + \left(\frac{\omega\epsilon}{\sigma}\right)^2} + \frac{\omega\epsilon}{\sigma}} \simeq \sqrt{\frac{2}{\omega\mu\sigma}} \quad \text{if } f \ll \frac{\sigma}{\epsilon} \quad (2.4)$$

In the table 2.2,[2] you could see the variation of some of these parameters with frequency and medium. In particular, the propagation distance has been calculated for a 100dB attenuation of a propagating plane wave as:

$$-\frac{20 \log \left(\frac{1}{e} \right)}{\delta_{skin}} = \frac{100dB}{distance} \tag{2.5}$$

Also, there's a comparison between the velocity of electromagnetic waves and acoustic waves; as you can see electromagnetic waves are much faster, thus explaining why they're used instead of acoustic waves when low latency is needed.

		Frequencies (Hz)					
		100	1k	10k	100k	1M	10M
Propagation velocity (m/s)	Sea water	$1.77 * 10^4$	$4.88 * 10^4$	$1.52 * 10^5$	$4.82 * 10^5$	$1.52 * 10^6$	$4.30 * 10^6$
	Fresh water	$3.16 * 10^5$	$1.00 * 10^6$	$3.16 * 10^6$	$1.00 * 10^7$	$3.16 * 10^7$	$1.00 * 10^8$
	Free space	$3.00 * 10^8$	$3.00 * 10^8$	$3.00 * 10^8$	$3.00 * 10^8$	$3.00 * 10^8$	$3.00 * 10^8$
	Acoustic	$1.50 * 10^3$	$1.50 * 10^3$	$1.50 * 10^3$	$1.50 * 10^3$	$1.50 * 10^3$	$1.50 * 10^3$
Wavelegth (m)	Sea water	$1.76 * 10^2$	$4.88 * 10^1$	$1.52 * 10^1$	$4.82 * 10^0$	$1.52 * 10^0$	$4.30 * 10^{-1}$
	Fresh water	$3.16 * 10^3$	$1.00 * 10^3$	$3.16 * 10^2$	$1.00 * 10^2$	$3.16 * 10^1$	$1.00 * 10^1$
	Free space	$3.00 * 10^6$	$3.00 * 10^5$	$3.00 * 10^4$	$3.00 * 10^3$	$3.00 * 10^2$	$3.00 * 10^1$
Propagation distance (m) for a 100dB attenuation	Sea water	$3.23 * 10^2$	$8.92 * 10^1$	$2.79 * 10^1$	$8.81 * 10^0$	$2.79 * 10^0$	$7.87 * 10^{-1}$
	Fresh water	$5.78 * 10^3$	$1.83 * 10^3$	$5.78 * 10^1$	$1.83 * 10^1$	$5.78 * 10^1$	$1.83 * 10^1$

Table 2.2: EM performance underwater [2]

2.3 EM waves propagation

After having described some of the parameters of electromagnetic waves, the propagation itself will be described.

2.3.1 Solution of Maxwell equations for elementary sources

The propagation of an electromagnetic wave is fully described by a set of equation called Maxwell equations. Using the assumption of homogeneity, linearity and isotropy of the medium, and harmonic regime, Maxwell equations could be written in this form:

$$\begin{aligned}
 \nabla_{\mathbf{x}} \underline{E} &= -j\omega\mu \underline{H} - \underline{M} \\
 \nabla_{\mathbf{x}} \underline{H} &= -j\omega\epsilon \underline{E} + \underline{J} \\
 \nabla \cdot \underline{H} &= \rho_m / \mu \\
 \nabla \cdot \underline{E} &= \rho_e / \epsilon
 \end{aligned} \tag{2.6}$$

In which:

\underline{E} is the phasor of the electric field;

\underline{H} is the phasor of the magnetic field;

\underline{M} is a fictitious quantity called magnetic current density;

\underline{J} is the electric current density;

ρ_m is a fictitious quantity called magnetic charge density;

ρ_e is the electric charge density

Finding a solution for these equations is most of the time quite complex. A simplification could be made when the source of the electromagnetic wave could be considered as a point source. In this case the solutions of Maxwell equations, expressed in a polar form are [7]:

$$\begin{aligned}
 \underline{E}(\underline{r}) &= -j \frac{\eta m_e}{r\lambda} e^{-\gamma r} \left[\left(\frac{j}{kr} + \frac{1}{(kr)^2} \right) \cos \theta \hat{r} + \frac{1}{2} \left(1 - \frac{j}{kr} + \frac{1}{(kr)^2} \right) \sin \theta \hat{\theta} \right] \\
 \underline{H}(\underline{r}) &= j \frac{m_e}{2r\lambda} e^{-\gamma r} \left(1 - \frac{j}{kr} \right) \sin \theta \hat{\phi}
 \end{aligned} \tag{2.7}$$

for an elementary dipole, which is an element with an electric current density represented by a Dirac δ . The quantity m_e is the electric moment of the dipole. If we consider, instead, an elementary magnetic element, whose magnetic current density will be represented as a Dirac δ as well and with a magnetic moment m_m , then the electric and magnetic fields will be given by:

$$\begin{aligned}
 \underline{H}(\underline{r}) &= -j \frac{m_m}{2r\lambda\eta} e^{-\gamma r} \left[\left(\frac{2j}{kr} + \frac{2}{(kr)^2} \right) \cos \theta \hat{r} - \left(1 - \frac{j}{kr} - \frac{1}{(kr)^2} \right) \sin \theta \hat{\theta} \right] \\
 \underline{E}(\underline{r}) &= -j \frac{m_m}{2r\lambda} e^{-\gamma r} \left(1 - \frac{j}{kr} \right) \sin \theta \hat{\phi}
 \end{aligned} \tag{2.8}$$

If we look closer at equations 2.7 and 2.8 we could see that the dependence of the fields from the radial distance r is given by the terms in the parenthesis, the intrinsic impedance and the exponential term. Let's consider the exponential term. The coefficient γ is given by one of the equations in 2.2. So, the exponent $-\gamma r$ will be equal to:

$$-\gamma r \simeq -jk_0 r \text{ in a dielectric medium;}$$

$$-\gamma r \simeq -\sqrt{j\omega\mu\sigma} = -\sqrt{\frac{\omega\mu\sigma}{2}}(1 + j) \text{ in a conductive medium.}$$

This means that the exponential term will have not only a phase term, but also an attenuation term which is proportional to the conductivity of the medium and to the frequency of operation.

2.3.2 Attenuation and choice of VLF

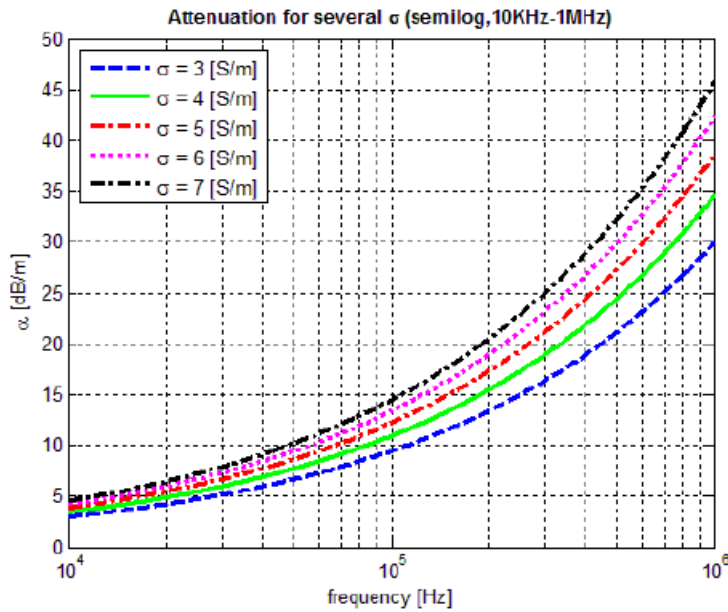


Figure 2.2: Attenuation of an EM wave as a function of frequency for different conductivities [8]

In figure 2.2 you could see the attenuation of an electromagnetic wave as a function of frequency and for different conductivities. These calculations were done

in [8] expressing the conductivity according to Weyl model. Our attempt in this project is to build a system whose range is of tens of meters. This means that, to have a decent quality of the signal, according to figure 2.2, we should work at a frequency below 20kHz. The operating frequency we've chosen is 10kHz. According to table 2.2, in this way we could reach a distance of around 28m with an attenuation of 100dB.

2.3.3 Multipath propagation

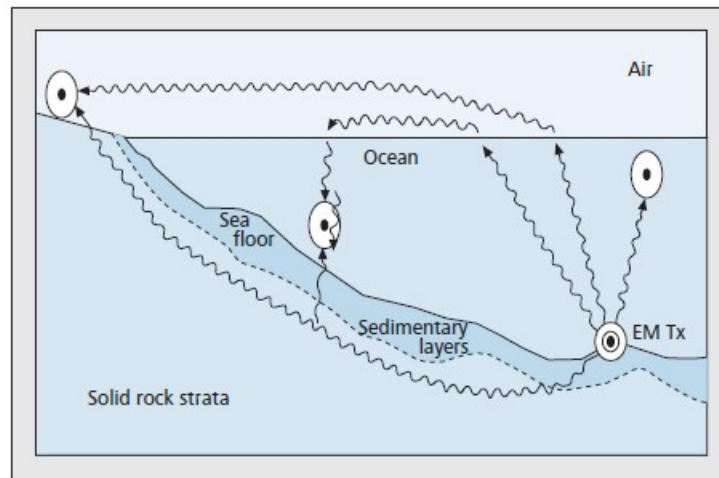


Figure 2.3: Multipath propagation in seawater [2]

It is important to considerate the effect of water-air and water-seabed boundaries when studying the performances of EM waves underwater. Because of the high permittivity, the wave experiences a large refraction angle, which leads to a transmission of the signal in a path almost parallel to the water. This way, it appears that the signal is radiated from a patch of water right above the transmitter. This effect greatly helps the transmission from a submerged station to the land or between shallow submerged station without the need for a surface repeater. A similar effect is produced by the seabed. The conductivity of the seabed is much lower than water, so it can provide a low-loss, low-noise alternative communication path. This is illustrated in figure 2.3. In many deployments the single propagation path with the least resistance will be dominant. Relatively longer transmission ranges could be

reached if the air path or seabed path should be chosen. Therefore, the multipath propagation of EM waves can be favourable for signal transmission in shallow water [2].

Chapter 3

Antenna and transmission

3.1 Antenna choice

The choice of the antenna has been made to meet different requirements:

- It needed to be easy to fabricate and low cost;
- It needed to be compact;
- It needed to work fine at very low frequencies.

Starting from the first requirement, the easiest antennas to be fabricated are dipole antennas or loop antennas. The former is made of a couple of conductive elements, or rods, fed in the center by a balanced transmission line (figure 3.1). The currents on the two rods have same module, but flow in opposite ways [1].

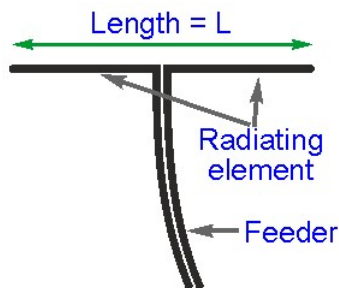


Figure 3.1: Dipole antenna [10]

The latter is made by a conductive wire which could be of different shapes: triangular, square, circular shaped loop antennas have been designed. However, the circular antenna (figure 3.2) is the one which has drawn most of the attention, hence most of the works are done with this particular shape.

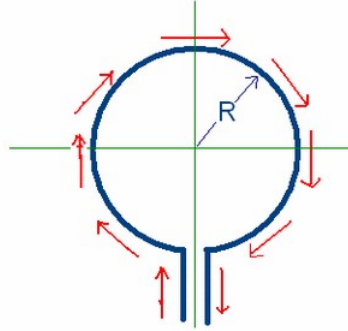


Figure 3.2: Circular loop antenna [11]

Both these antennas are easy to fabricate, low cost and flexible. Since we are going to work at low frequencies, the size requirement is pretty strict: the goal is to design a system which is going to work with an antenna whose diameter is not exceeding 15cm. This means that the antennas will be short with respect to the wavelength and their performances will be inferior compared to a larger antenna. A way to increase the loop performance is to create a multi-loop antenna; adding more loops will enlarge the magnetic field of the loop, thus enhancing the performances of the single one. Also, increasing the number of loops does not affect the compactness of the antenna in a significant way. Besides, the magnetic field transmitted by a loop antenna could be further increased by adding a ferrite element at the center of the coil [3]. For these reasons we decided to work with a loop antenna.

3.2 Near field operation and transmission equations

When working with antennas, often the "far field" approximation is used. The far field region for electrically short antennas is the one for which:

$$kr = 2\pi \frac{r}{\lambda} \gg 1 \quad (3.1)$$

Which means that being in far field region depends only on the distance and frequency of operation and not on the dimension of the antenna [7]. Referring to table 2.2, we could see that in sea water the wavelength of a EM wave at a frequency

of 10kHz is $\lambda = 15.2m$ while the 100dB attenuation range is $r = 27.9m$. Hence, the two quantities are of the same order of magnitude, so we could expect to work in a region called "near field" or, at most, in the "transition" region. This involves that, in the characterization or design of the antenna, we can not use some of the classical parameters which are defined in far field (for instance gain and directivity). This means that we can't use the Friis equation for the propagation to evaluate the amount of power received by an antenna given the power injected in the transmitting antenna. Moreover, we can not even define the radiation resistance: in free-space this involve obtaining an expression for the power flow through a spherical surface and dividing this by the square of the current which creates that power flow. In a conducting medium, however, you find that the expression for the total power crossing a sphere of radius R is a function of R unlike the free-space case in which is independent of R. Therefore, the evaluation of the radiation resistance, so useful for the antenna design, becomes impractical for a conducting medium. Intuitively, it is reasonable that the power flow depends on R: working in a conductive medium, the electromagnetic wave is continuously attenuated as it propagates through the dissipative region. Besides, the $1/r^2$ term, which is usually linked to a reactive power, is instead a real power loss, since not all the power leaving the antenna is coming back at each cycle but is lost in the medium [3]. What we can do is designing the transmitting antenna in order to achieve a certain voltage amplitude in the receiving antenna using the equations that link the magnetic flux to the induced electromagnetic force (e.m.f.) [3]. Considering two loop antennas whose radius is much lower than the wavelength of the operation frequency, the radiated magnetic field is given in equations 2.8. Let's suppose that the two loops are aligned to maximize the θ component ($\theta = 90^\circ$), which also means that the radial component will be 0; the magnetic flux density at a distance r from the transmitting loop is:

$$B_\theta = \mu_0 H_\theta \tag{3.2}$$

and the magnetic flux through the second loop will be:

$$\Phi_2 = B_\theta S_2 \tag{3.3}$$

In which S_2 is the surface of the second loop. Hence, assuming harmonic regime,

the induced e.m.f. will be

$$e.m.f. = -\frac{d\Phi_2}{dt} = -j\omega\Phi_2 \quad (3.4)$$

Applying these equations to 2.8 we obtain that the maximum e.m.f. induced in the second loop is given by

$$e.m.f._{max} = -\omega\mu_0 S_2 \frac{m_m}{2r\lambda\eta} e^{-\gamma r} \left(1 - \frac{j}{kr} - \frac{1}{(kr)^2} \right) \quad (3.5)$$

Supposing that the first loop is fed by a current I and has a surface S_1 then the magnetic moment of the loop will be given by

$$m_m = j\omega\mu I S_1 \quad (3.6)$$

we obtain the final expression:

$$\begin{aligned} e.m.f._{max} &= j\omega^2\mu_0^2 I S_1 S_2 \frac{1}{2r\lambda\eta} e^{-\gamma r} \left(1 - \frac{j}{kr} - \frac{1}{(kr)^2} \right) \\ &= \omega^2\mu_0^2 I S_1 S_2 \frac{1}{2r\lambda\eta} e^{-\gamma r} \left(j + \frac{1}{kr} - \frac{j}{(kr)^2} \right) \end{aligned} \quad (3.7)$$

A way to increase the magnetic field coupling of the two loops (which means increasing the radiated field and the induced e.m.f) is using multi-turn antennas and ferrite loaded antennas. A multi-turn antenna is simply an antenna with more than one winding. If a loop antenna has N turns, it could be described as an equivalent single turn antenna with a surface N times larger. This means that, if the transmitting antenna and the receiving antenna are identical, the induced e.m.f. on the receiving antenna will be increased of a factor N^2 . A ferrite loop antenna is a loop antenna wound on a ferrite core which has high magnetic permeability in the operating frequency. Large magnetic permeability means large magnetic flux and therefore a larger induced e.m.f.. However, the magnetic permeability of the material is always higher than the effective magnetic permeability that is taken into account in the transmission equation. The ratio between the former and the latter strongly depends on the geometry of the ferrite. Toroidal cores have the highest effective magnetic permeability, while ferrite-stick cores have the lowest. In figure 3.3 you could see an example of effective magnetic permeability in ferrite rods as a function

of the length-to-diameter ratio and with material permeability as a parameter. If we suppose to have two identical, ferrite loaded antennas, with an effective magnetic permeability $\mu_{r_{eff}}$ then the induced e.m.f. would be increased by a factor $\mu_{r_{eff}}^2$

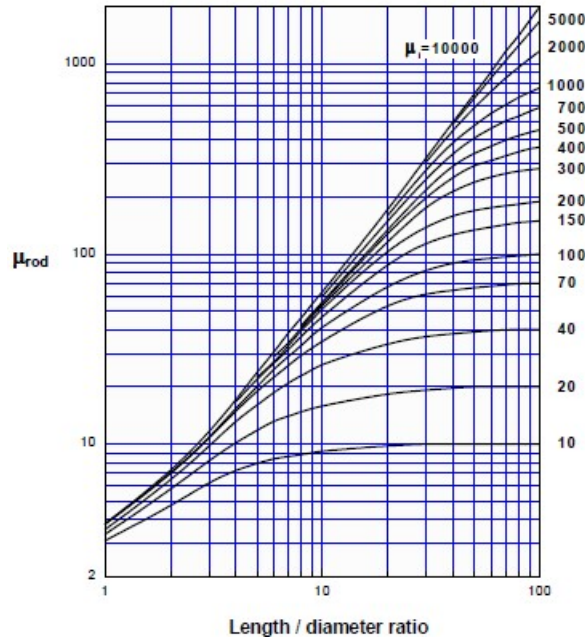


Figure 3.3: Effective magnetic permeability in ferrite rods as a function of the length-to-diameter ratio and material permeability

3.3 Circuit modelling of a loop antenna

In literature there are several circuit models of a loop antenna. In [9] an eight lumped elements model is described (figure 3.4). Starting from a five lumped elements model for an antenna in free space, the eight lumped elements is derived as in [12] to evaluate the effect of a conductive medium on the antenna; it has been shown that in a conductive medium the resistors become inductive, while the capacitors become conductive. To evaluate the starting five elements model the first two resonance frequencies are needed to evaluate the values of capacitances and inductors, while the resistance is given by the sum of radiation resistance and loss resistance. Then, considering that in a conductive medium the permittivity is a complex number, the capacitances will be given by:

$$C = C_0(1 - j \tan \delta) \quad (3.8)$$

where $\tan \delta = \frac{\sigma}{\epsilon_0 \epsilon_r \omega}$ is called loss tangent. The resistance will be:

$$R = \frac{R_0}{\sqrt{1 - j \tan \delta}} \quad (3.9)$$

A rougher but easier-to-use method to model the antenna is considering it as a lossy inductor (figure 3.5 [13]). The total resistance is given by the sum of the radiation resistance and of the resistance of the wire, while the inductance is given by the sum of the loop inductance and of the wire inductance. In this case the wire inductance and the radiation resistance could be neglected, so the values of resistance and inductance of the loop could be evaluated as:

$$\begin{aligned} R_l &= \frac{4\rho N c_1 \sqrt{S}}{\pi d^2} \\ L_a &= 2.00 \cdot 10^{-7} N^2 c_1 \sqrt{S} \left(\ln \frac{c_1 \sqrt{S}}{\sqrt{N} d} - c_2 \right) \end{aligned} \quad (3.10)$$

In which:

ρ is the resistivity of copper;

d is the diameter of the wire;

c_1 and c_2 are constants related to the geometry of the loop.

A figure of merit of such a circuit is the quality factor Q . This parameter is a measure of the losses of the inductor itself and is defined as:

$$Q = \omega \frac{\text{energy stored}}{\text{average power dissipated}} = \omega \frac{L_a}{R_l} \quad (3.11)$$

The higher the quality factor, the higher the amount of the energy stored in the inductor with respect to the losses.

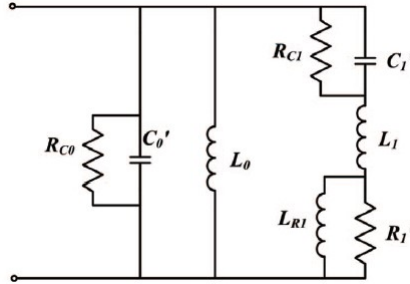


Figure 3.4: Eight lumped elements model of a magnetic antenna

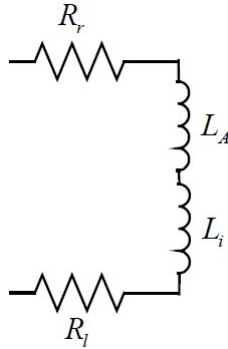


Figure 3.5: Loop antenna as lossy inductor

3.4 Measurements on the antenna

To test the first prototype of the system we didn't design an antenna, but we used an antenna already in our laboratory. In figure 3.6 a picture of the antenna is shown. To characterize it we used the impedance analyzer AGILENT 4294a. The results of the measurements in free air are shown in figure 3.7 and 3.8. We were interested in a range around the operational frequency, so the measures were taken in the range $1kHz - 100kHz$.

The antenna shows an inductance $L_a = 9.15mH$ and a resistance $R_l = 28.8\Omega$ at $f = 10kHz$. The quality factor is $Q = 20$. In figure 3.9 you can see the behaviour of the module and phase of the input impedance. At the frequency range of interest, the antenna behaves as an inductor with losses, as you can see from the module of the impedance growing 20dB/dec and from the almost 90° phase rotation. This



Figure 3.6: A picture of the antenna used

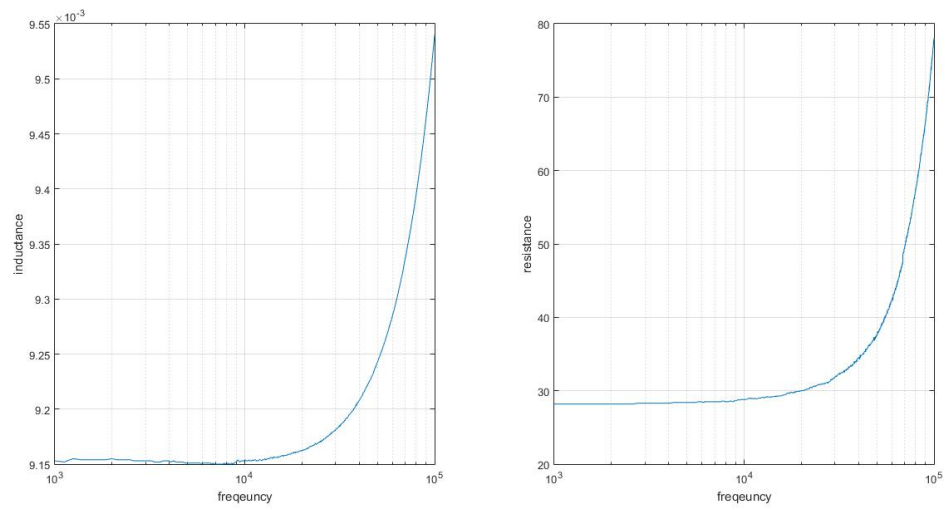


Figure 3.7: Inductance and resistance of the antenna vs frequency

means that, at least in air, which is a lossless medium, we can model the antenna as an inductor with losses.

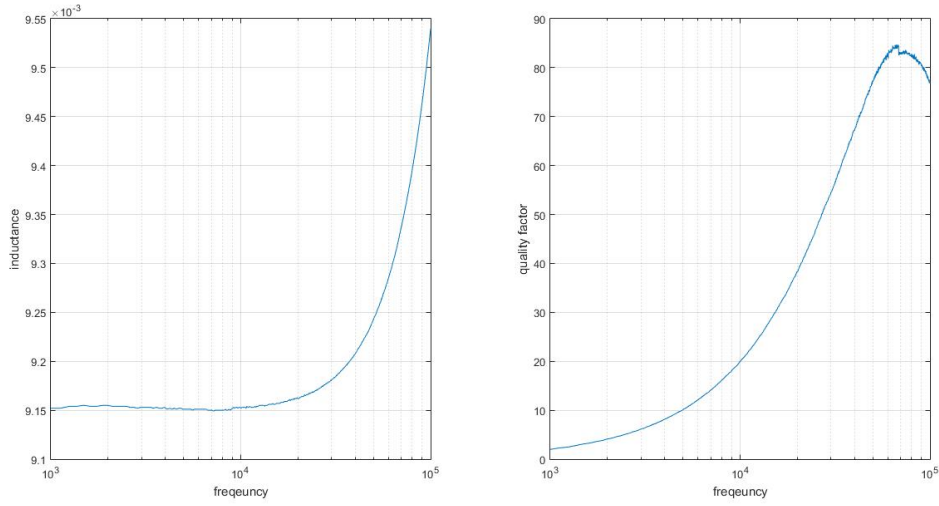


Figure 3.8: Inductance and quality factor of the antenna vs frequency

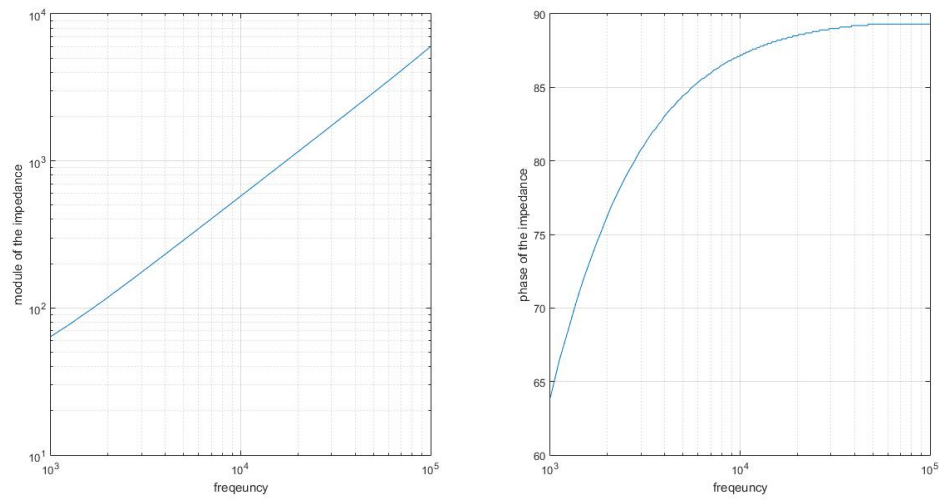


Figure 3.9: Module and phase of the antenna impedance vs frequency

Chapter 4

The system

In this chapter the designed system will be described. An overview of the system is shown in figure 4.1. The transmitting part consists in a signal generator, implemented on the development board Arch Max, which generates a sine wave at a frequency of 10kHz. This signal is amplified by a power amplifier and sent to the antenna, which is connected in series to a capacitor to resonate at the operational frequency. This allows the maximum power transmission. The receiving part consists in the receiving antenna, which resonates with a parallel capacitor; a first stage of rough filtering with a differential second order band pass filter; a low noise amplifier; finally, another filtering stage, a fourth order band pass Butterworth filter. The signal is then sent to the ADC of the development board.

4.1 The Arch Max development board

The Arch Max is a development board for rapid prototyping (figure 4.2). The microcontroller on this board is a STM32F407VET6, based on ARM Cortex-M4 32-bit. The board has been programmed to generate a sine wave at a frequency of 10kHz and output it on one of the two DAC channel [14]. Also, the board will provide some of the control signals needed by other components in the system. Finally, it will be used to receive the signal after the receiving chain. To this aim, the 12-bit ADC is used. The board works with a power supply of 3.3V, but it is powered at 5V; then it has an internal linear regulator to regulate the voltage at 3.3V. The linear regulator is dissipative, which means lower efficiency in powering the board. Since the 5V are not needed in normal operation of the board, the regulator has been bypassed and the board powered with a 3.3V generated by an external switching regulator (see section 4.4).

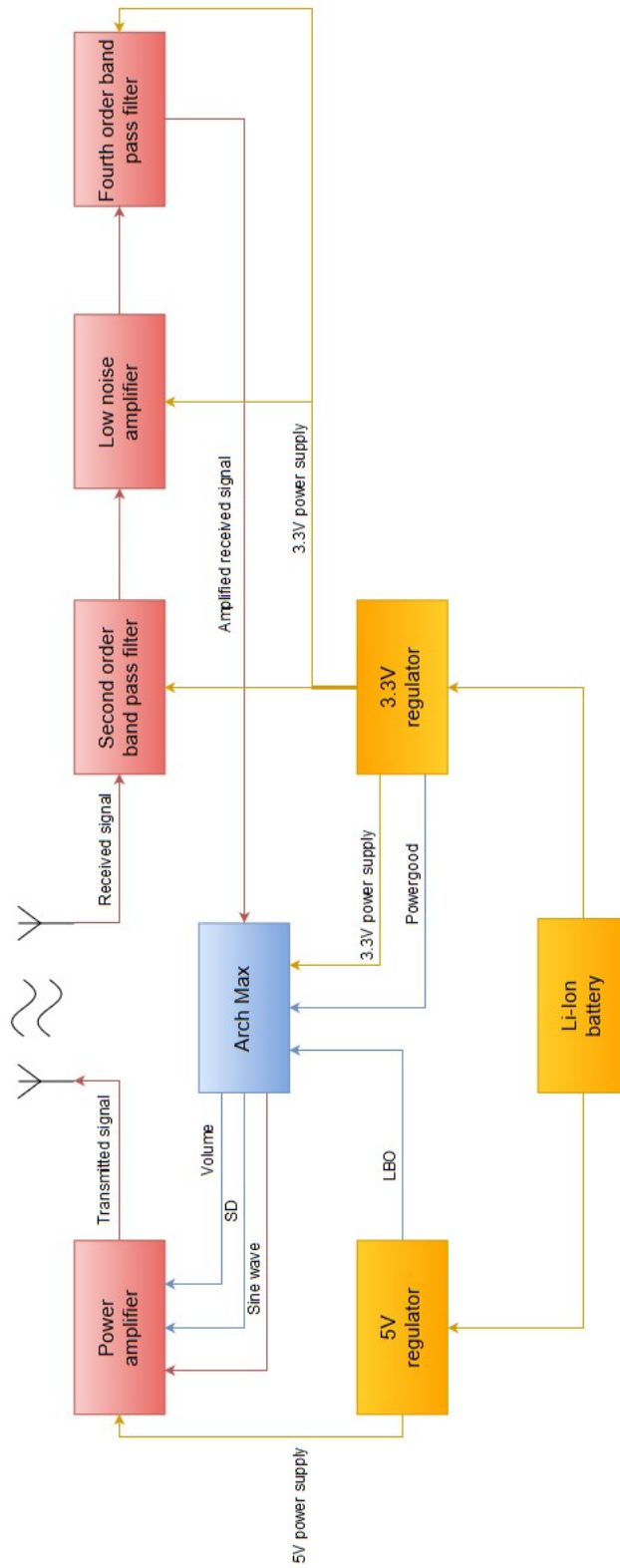


Figure 4.1: System block diagram

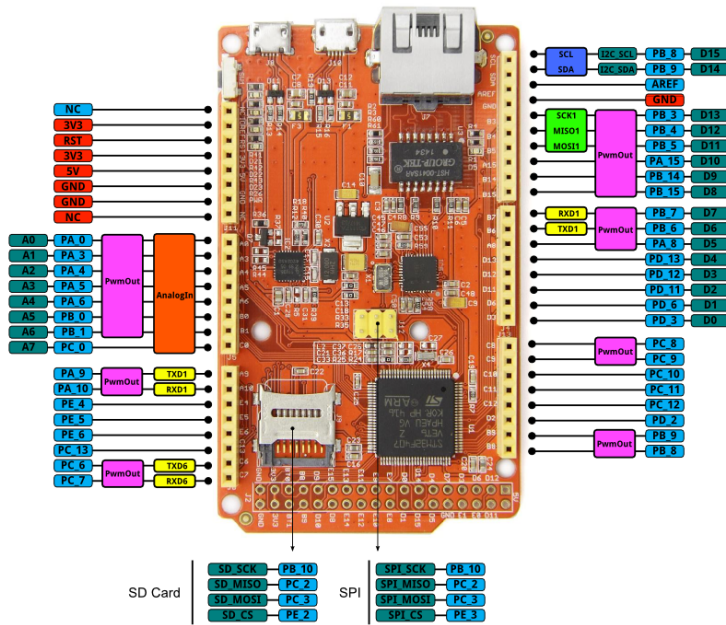


Figure 4.2: Arch Max

4.2 The transmitter

The signal generated by the Arch Max has to be amplified to properly feed the transmitting antenna. The transmitter has to deal with high power signal, so a amplifier that can efficiently deal with high power is needed. A class D amplifier was chosen.

4.2.1 Class D amplifiers

In class D amplifiers the transistors are used just to steer the current through the load; this means that the power losses are much lower when compared to linear amplifier such as class A or AB amplifiers. The basic principle of operation of a half-bridge class D amplifier is shown in figure 4.3 [15]. The input signal is compared to a triangle wave to create a PWM driving signal for the transistor couple. If the switching frequency of the transistors is much higher than the input frequency, the harmonic content related to the input could be easily filtered out to obtain

the amplified output waveform. The power lost in the process is related to the transistor on-resistances, to the switching losses and to the quiescent currents. To further improve the efficiency, linearity, and the immunity to noise, this system is closed in a loop that senses the output voltage. For our purposes, a full-bridge class

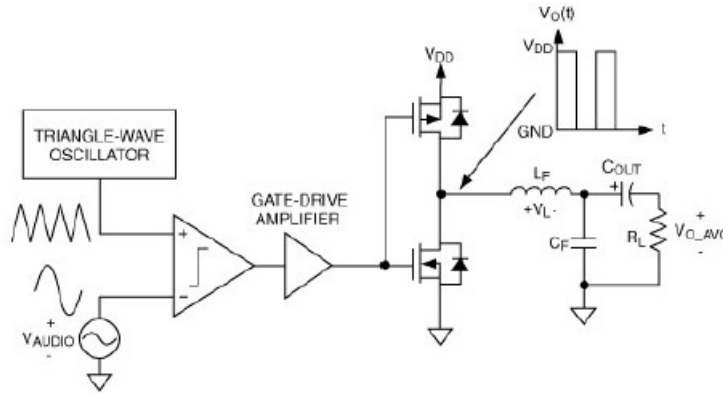


Figure 4.3: Class D basic operation [15]

D amplifier (figure 4.4) was preferable: it allows to double the output swing on the load keeping the same supply voltage. The number of transistor has doubled, which means more losses, but this is a concern when dealing with higher power than in this project.

4.2.2 Circuit design

The amplifier Texas Instruments TPA2008D2 has been chosen. The schematic of the circuit is shown in figure 4.5. The amplifier has a differential input and output but here a single ended input was needed, so one of the inputs was connected to ground through a capacitor. Extra components were needed for the internal oscillator, for the input filter and to bypass the supply voltage. The amplifier works with a 5V supply voltage, allowing efficiency up to 88% with a 8Ω load with low harmonic distortion. The volume pin could be used to regulate the gain. A SD pin is present, to allow the shutdown of the amplifier [16]. The output of the amplifier is connected to the antenna. Each output of this amplifier is a square wave; the two waves are in phase, but their duty cycles vary depending on the input voltage; hence, the output differential voltage will be given by voltage impulses whose width is proportional to

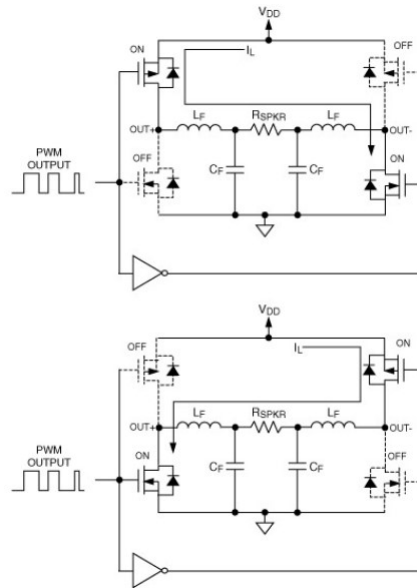


Figure 4.4: Class D full bridge operation [15]

the input voltage (figure 4.6). The antenna is put in series with a capacitor to make it resonate. The expected voltage across the antenna terminals is a sine wave whose amplitude will be determined by the gain of the amplifier and by the quality factor of the LC resonator.

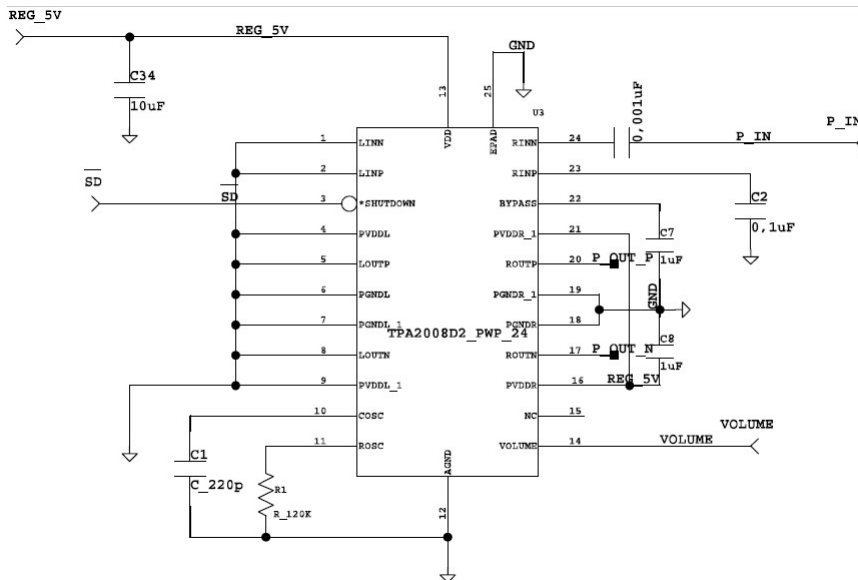


Figure 4.5: Schematic of the power amplifier

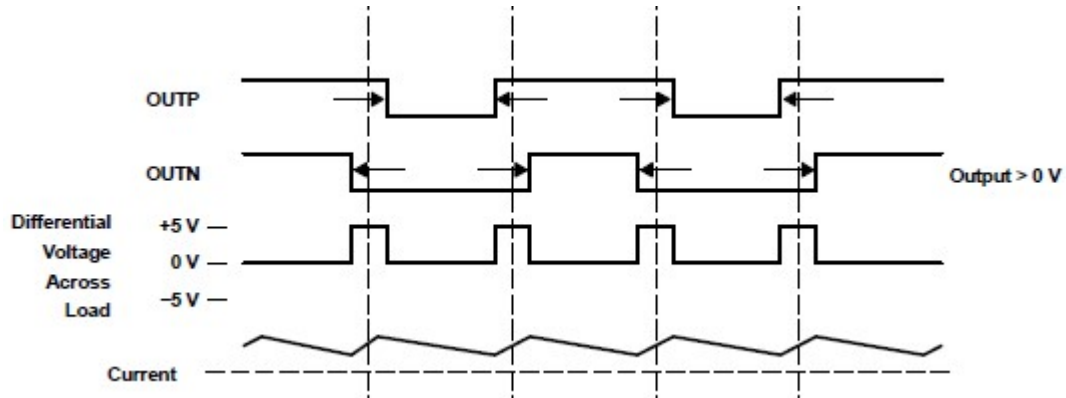


Figure 4.6: Amplifier output on an inductive load [16]

4.3 The receiver

The receiver deals with low voltage, noise sensitive signals. Therefore, some filtering stages and a low noise amplifier were needed. Also, to adapt the signal to the ADC dynamic, a high gain of the receiving chain is needed. The component we decided to use is the Texas Instruments TLV4376 low noise amplifier. In the package there are four low noise operational amplifier, with a gain-bandwidth product of $5.5GHz$, a input referred voltage noise density of $8nV/\sqrt{Hz}$ and a input referred current noise density of $2fA/\sqrt{Hz}$ [17]. In figure 4.7 you can see the schematic of the circuit.

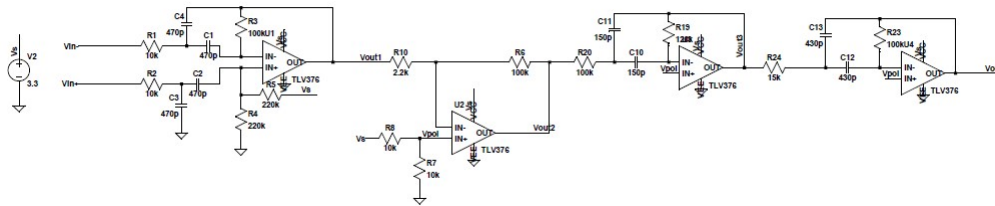


Figure 4.7: Schematic of the receiver

4.3.1 Circuit design

The first stage is an active band pass filter with a differential input. This stage was inserted to cut the noise band before the amplification. The transfer function of a

second order band pass filter is in the form:

$$H_{bp} = H_0 \frac{\frac{\omega_0}{Q} s}{s^2 + \frac{\omega_0}{Q} s + \omega_0^2} \quad (4.1)$$

To design the filter, a multi-feedback (MFB) cell has been used. Referring to the first stage of figure 4.7, the transfer function of the filter is:

$$H_1 \simeq \frac{sC_1R_3}{s^2C_1C_4R_1R_3 + sR_1(C_1 + C_4) + R_1} \quad (4.2)$$

Comparing 4.1 and 4.2 it can be seen that:

$$\begin{aligned} \omega_0 &= \frac{1}{C_1C_4R_1R_3} \\ Q &= \frac{1}{2} \sqrt{\frac{R_3}{R_1}} \\ H_0 &= \frac{R_3}{2R_1} \end{aligned} \quad (4.3)$$

Components of the series E12 have been used. With the values shown in figure 4.7 we obtained:

$$\begin{aligned} f_0 &= 10.7kHz \\ Q &= 1.58 \\ H_0 &= 5 \end{aligned} \quad (4.4)$$

In figure 4.8 you can see the result of the simulation in LtSpice.

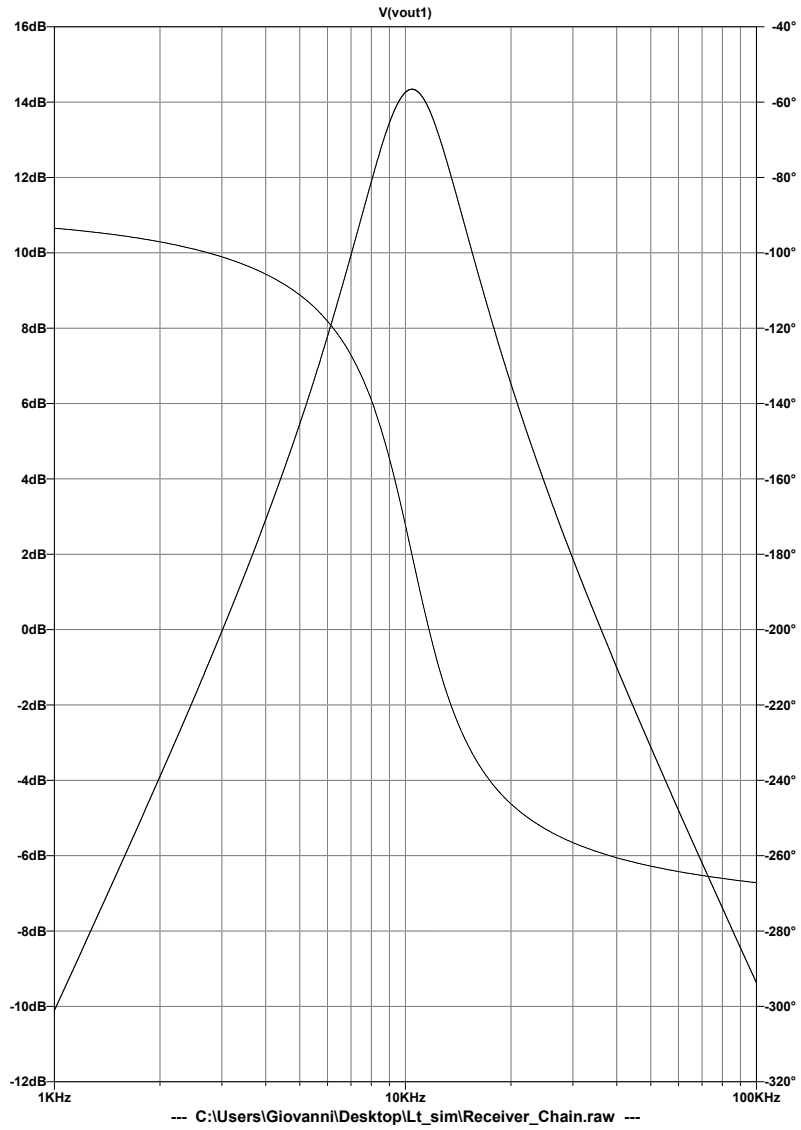


Figure 4.8: Frequency response of the first filter

The stability of the filter has been analysed. In figure 4.9 the closed loop gain of the circuit is shown. It can be seen that at the crossover frequency, the phase of the loop gain is around 70° . This means that the circuit is stable.

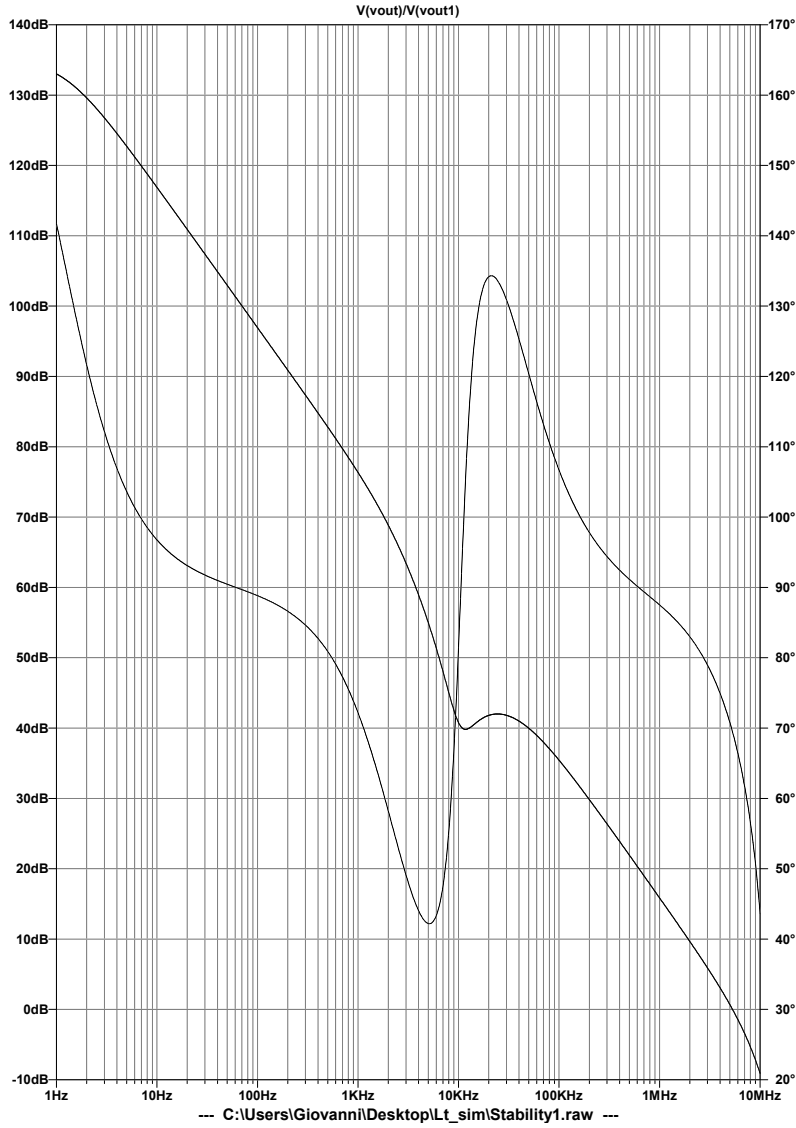


Figure 4.9: Closed loop gain of the first filter

The second stage is an inverting amplifier. The gain is fixed, but in the realization of the circuit different resistances could be used to vary it. In the simulations, the gain has been set to the maximum. The maximum gain that a single stage can achieve is set by the gain-bandwidth product of the opamp; assuming that the bandwidth of the system has to be at least one decade higher than the working frequency:

$$G_{max} = \frac{GBW}{100kHz} = 51 \quad (4.5)$$

The transfer function of this stage is:

$$H_2 = -\frac{R_6}{R_{10}} = -45.45 \quad (4.6)$$

Finally, another filtering stage is added. This time a fourth order filter Butterworth is designed, cascading two second order filter designed with MFB cells. A Butterworth filter is characterized by this transfer function:

$$|H| = \frac{1}{\sqrt{1 + \left(\frac{f}{f_c}\right)^{2n}}} \quad (4.7)$$

In which n is the order of the filter and f_c is the $-3dB$ frequency. This kind of filters are also called "maximally flat" because they have no in-band oscillation and a steep transition between pass band and attenuation band. To design such filters, design table are given, from which the polynomials to be designed are taken. The fourth order Butterworth polynomial is:

$$B_4(s) = (s^2 + 0.7654s + 1)(s^2 + 1.8478s + 1) \quad (4.8)$$

Which means that the two cascaded band pass stages should have these transfer functions:

$$\begin{aligned} H_3(s) &= \frac{0.7654s}{s^2 + 0.7654s + 1} \\ H_4(s) &= \frac{1.8478s}{s^2 + 1.8478s + 1} \end{aligned} \quad (4.9)$$

The circuit has been design comparing the two transfer functions and equation 4.1 and setting the central frequency at 10kHz. In figure 4.10 the frequency response of this stage is shown. The parameters of the filter as measured from the simulation are:

$$\begin{aligned} f_0 &= 9.6kHz \\ Q &= 1.92 \\ H_0 &= 2 \end{aligned} \quad (4.10)$$

The two stages have been analysed from the stability point of view. The results are shown in figure 4.11 and 4.12. Also in this case the phase of the loop gain is

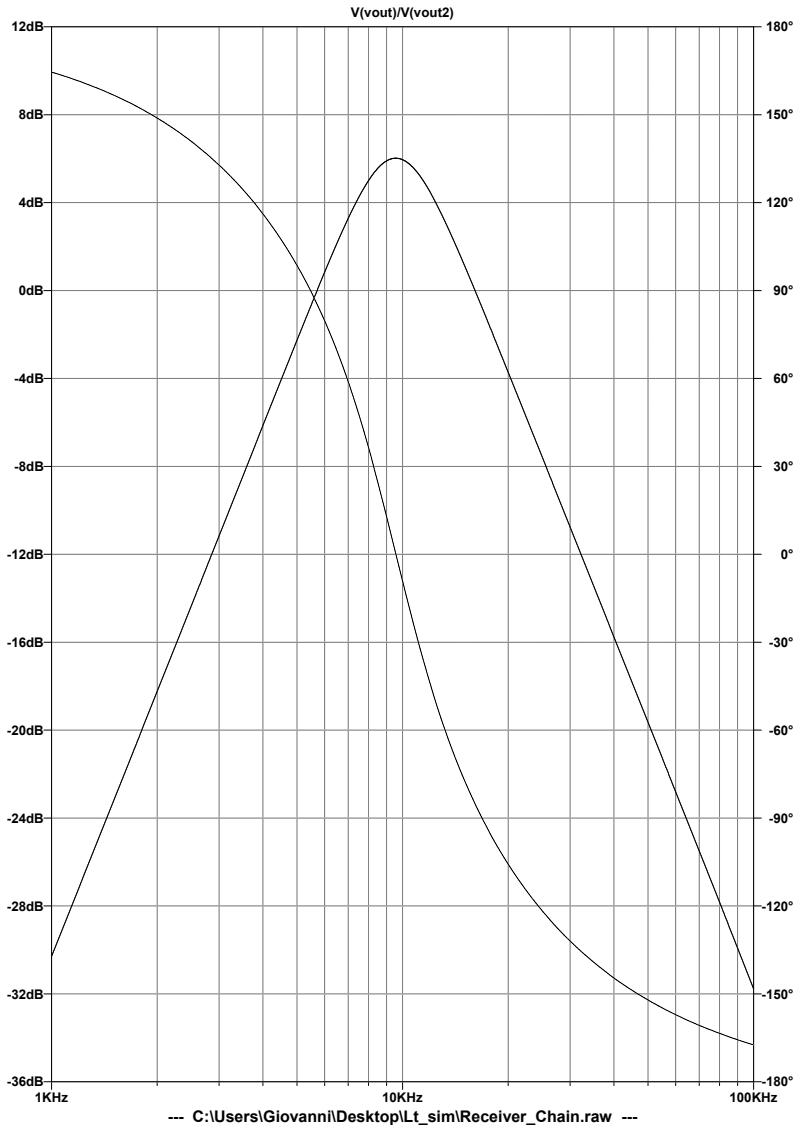


Figure 4.10: Frequency response of the second filter

much lower than 180° hence we can state that the circuit is stable. The parameters of whole circuit obtained from the simulation, whose result is shown in figure 4.13 are:

$$\begin{aligned}
 f_0 &= 10.02 \text{ kHz} \\
 Q &= 2.28 \\
 H_0 &= 465 \rightarrow 53.35 \text{ dB}
 \end{aligned}
 \tag{4.11}$$

Finally, a transient analysis has been performed, varying the frequency of the input waveform and with a peak amplitude of $1mV$. The results are shown in figures 4.14, 4.15, 4.16. In all the cases, an initial settling time in which a 10kHz waveform appears is required, but after that the signals out of band are attenuated.

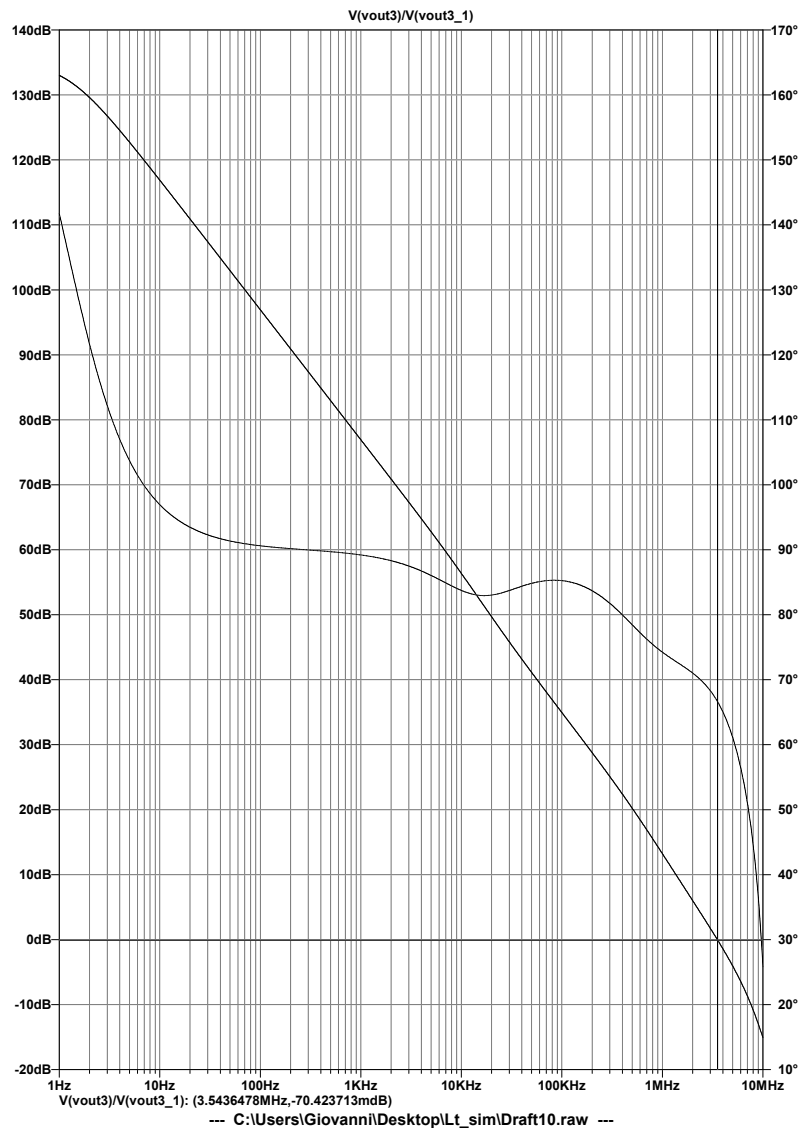


Figure 4.11: Closed loop gain of the second filter

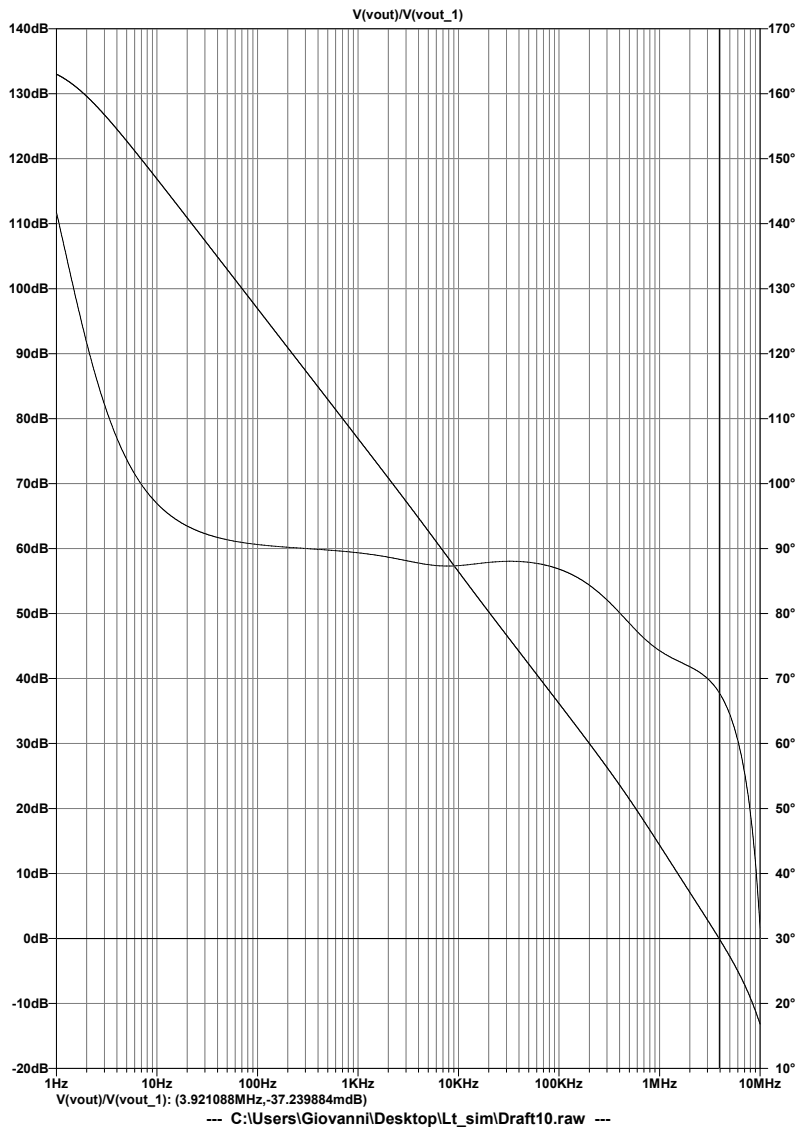


Figure 4.12: Closed loop gain of the third filter

4.3 – The receiver

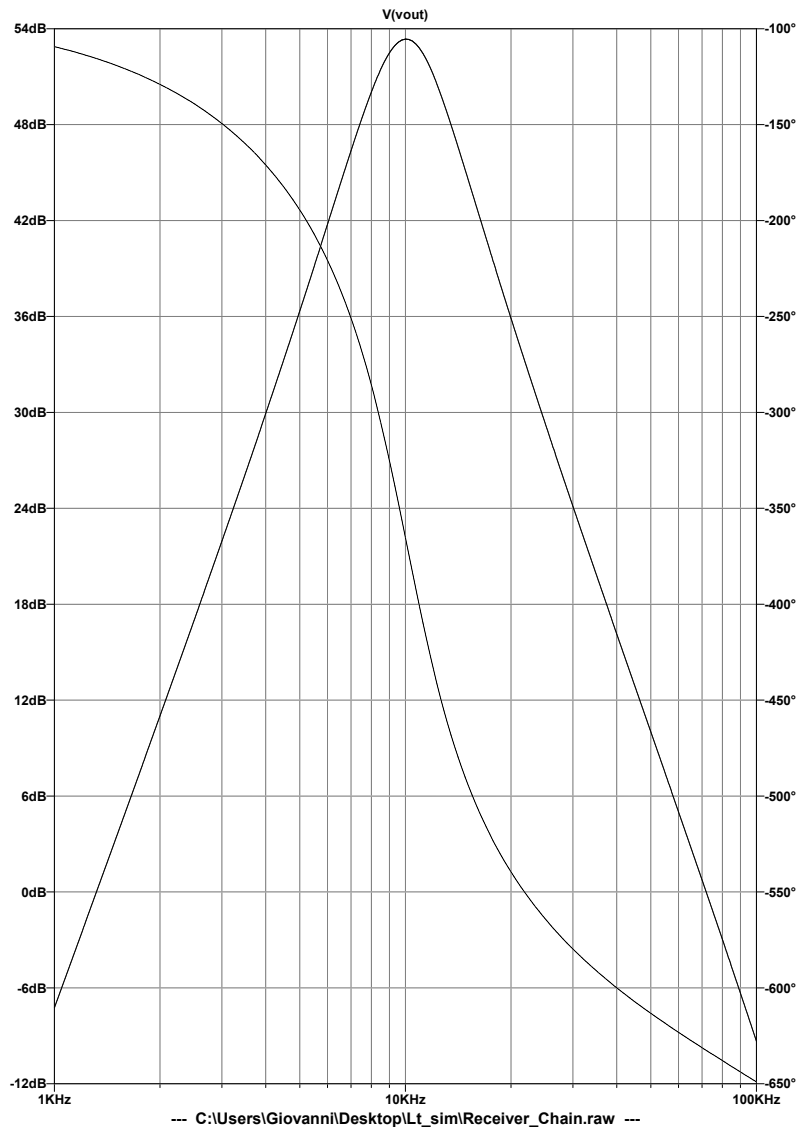


Figure 4.13: Frequency response of the circuit

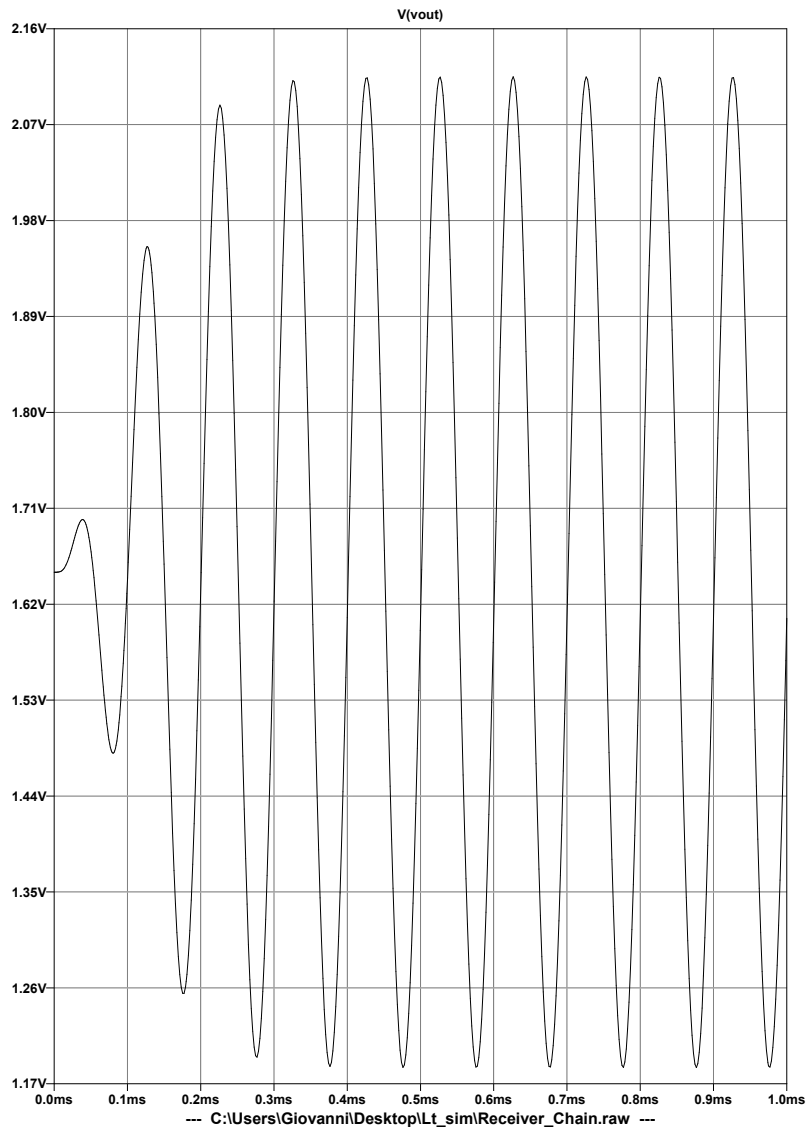


Figure 4.14: Output waveform with a 10kHz input

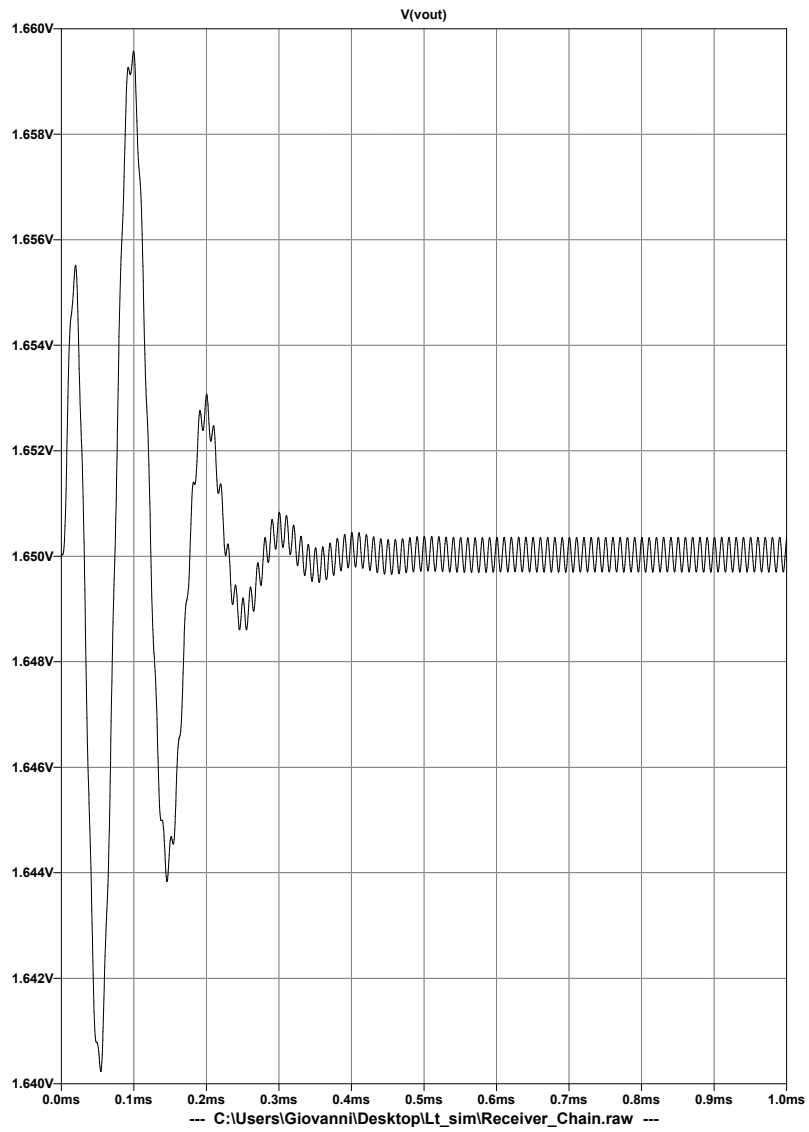


Figure 4.15: Output waveform with a 100kHz input

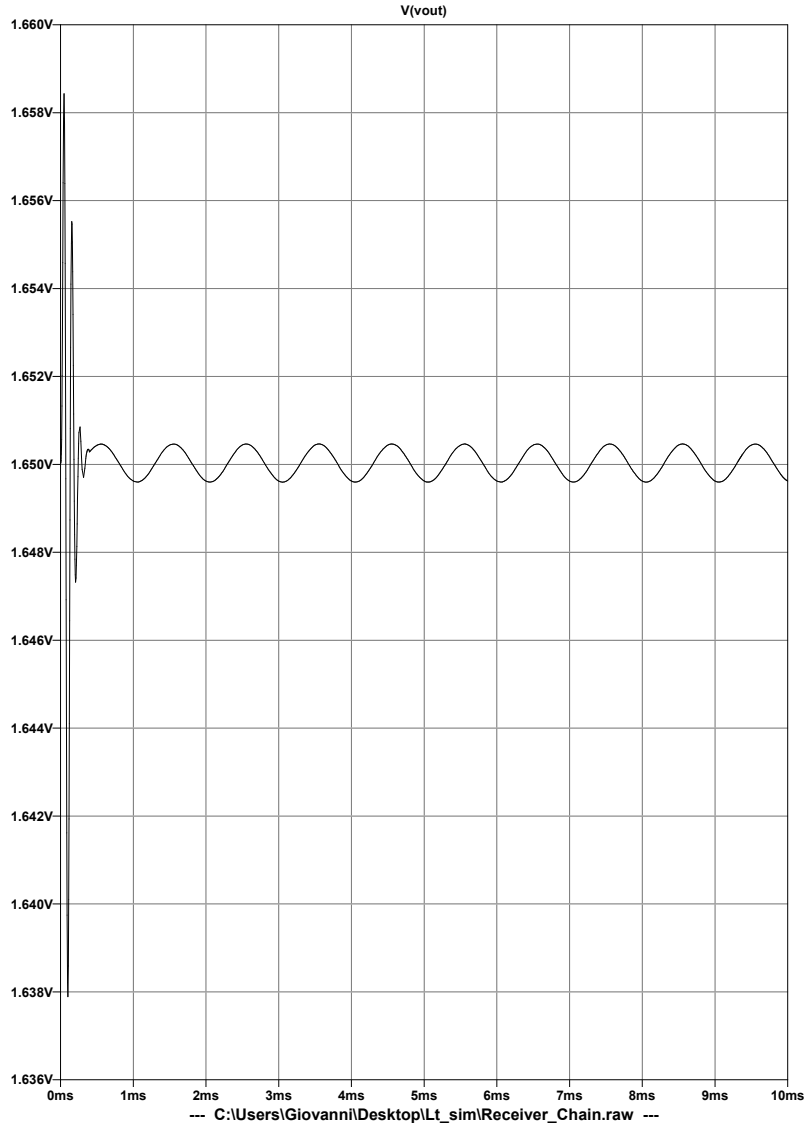


Figure 4.16: Output waveform with a 1kHz input

4.3.2 Sensitivity and input range of the circuit

The sensitivity of the receiver is set by two major factors: the precision of the ADC and the noise generated by the antenna. Knowing that the Arch Max has a 12-bit ADC powered by 3.3V, the minimum voltage allowed at its input is:

$$V_{out_{min}} = V_{LSB} = \frac{V_{ref}}{2^{12} - 1} = 0.81mV \quad (4.12)$$

This means that the sensitivity of the receiver is

$$V_{in_{min}} = \frac{V_{LSB}}{G} = 1.7\mu V \quad (4.13)$$

The noise generated by the antenna, instead, is essentially the thermal noise related to the antenna resistance. If a 28.8Ω loss resistance is assumed, then, since the input impedance of the first stage is much higher than this resistance, the input noise at a temperature of 300K is given by:

$$V_{noise} = \sqrt{4kTR_a} = 0.69nV/\sqrt{Hz} \quad (4.14)$$

In which k is the Boltzmann constant. Also, the noise figure of the circuit has to be considered. A noise analysis has been performed, finding the output noise of the circuit. The result is shown in figure 4.17. The expected noise figure can be evaluated:

$$NF = SNR_{in} - SNR_{out} = 10 \log \left(\frac{G^2 N_{in} + N_{circuit}}{G^2 N_{in}} \right) = 32.5dB \quad (4.15)$$

In which SNR stands for signal to noise ratio at the input and output of the receiver and N_{in}, N_{out} the noise density at the input and output of the receiver. The noise figure is high, but it was expected since a lot of resistances have been used. Now we can evaluate the sensitivity of the receiver related to the noise; assuming that, for a good error probability in a OOK modulation, $SNR_{out} = 12dB$ [20]

$$\begin{aligned} P_{in_{min}} [dB] &= 10 \log(4kTR_a BW) + NF + SNR_{out} = -105.7dB \\ V_{in_{min}} &= 10^{\frac{P_{in_{min}}}{20}} = 5.2\mu V \end{aligned} \quad (4.16)$$

Hence, the sensitivity of the system is limited by the noise.

The maximum voltage allowed at the receiver input is:

$$V_{in_{max}} = \frac{V_{ref}}{G} = 7.1mV \quad (4.17)$$

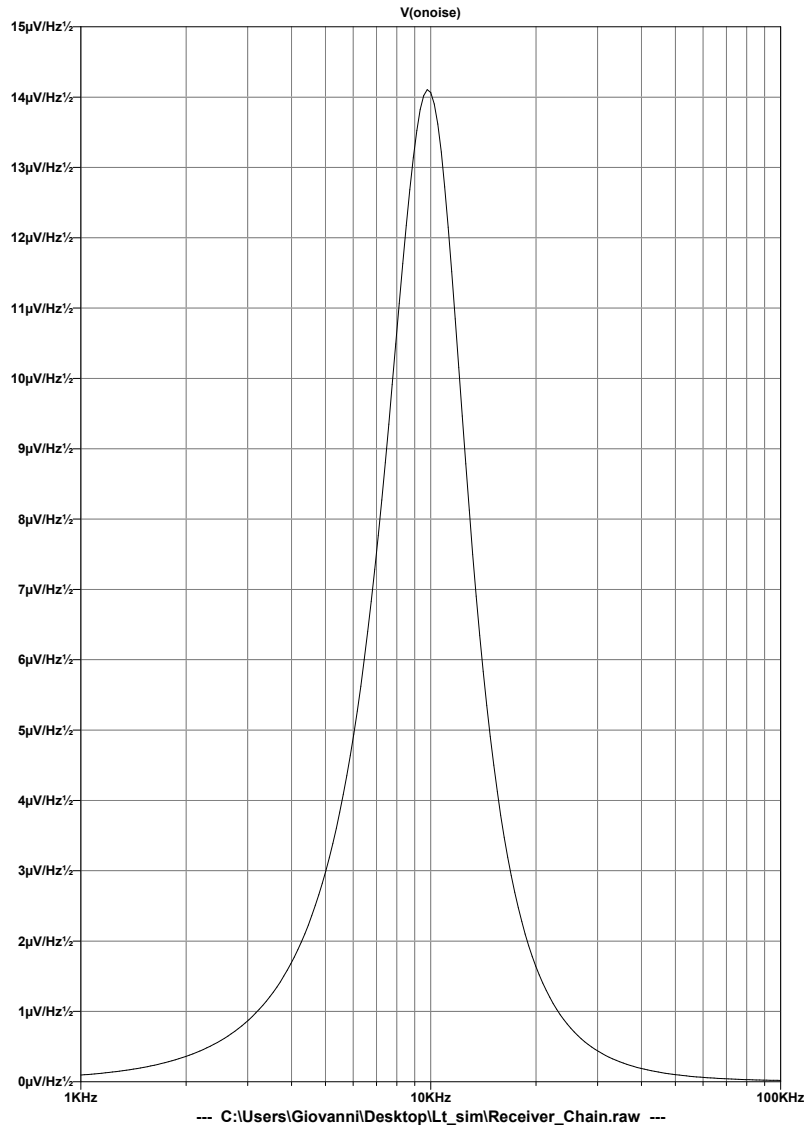


Figure 4.17: Output noise of the circuit

4.4 The power supply

In the system two power supplies are needed: a 5V power supply for the transmitting part, which needs to deal with high currents; a 3.3V power supply for the receiver and the board, with lower currents. The whole system will be powered by a Li-Ion 3.6V battery. So, a boost converter and a buck converter are needed. Switching

regulators have been chosen for efficiency reason. The boost converter is the Texas Instruments TPS61032. This converter outputs a fixed 5V voltage and a maximum current above 2A with an efficiency above 90%. The LBO control pin allows to check the state of the battery [18]. The schematic of the circuit is shown in figure 4.18. Most of the components were chosen following the suggestions on the datasheet,

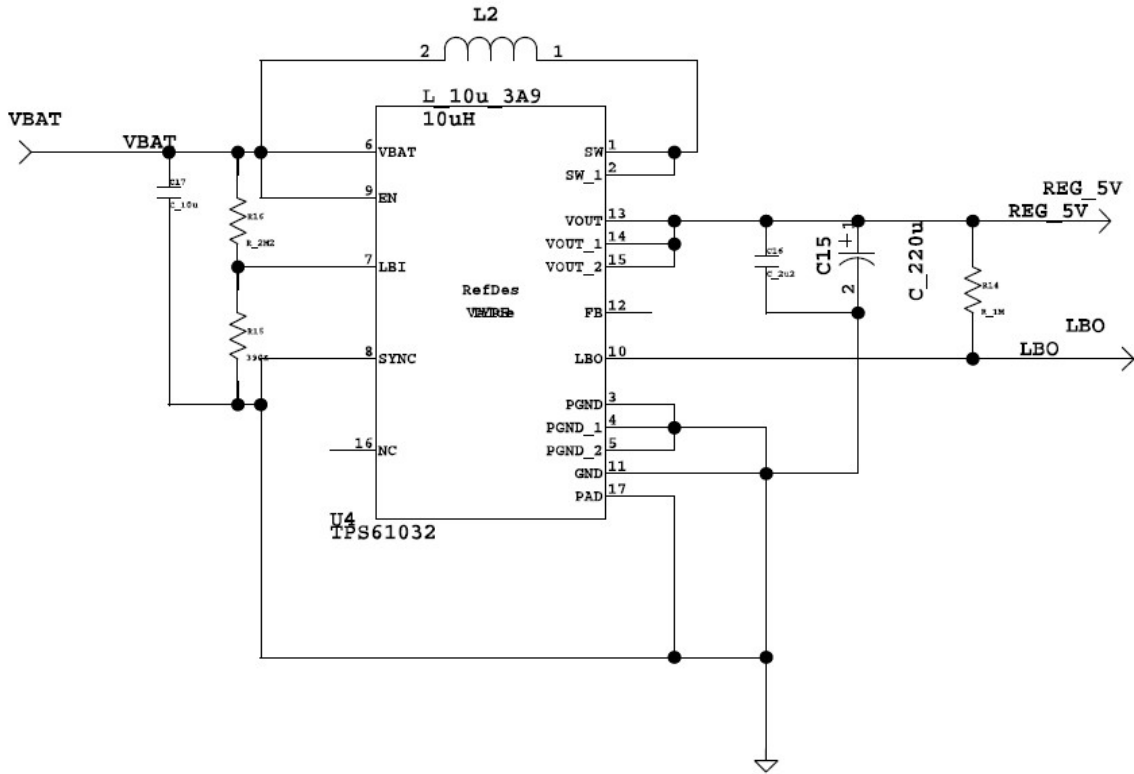


Figure 4.18: Schematic of TPS61032

[18], but the inductor and the resistances R_{15} and R_{16} were chosen to meet specific requirements in this project. The resistances set the threshold for which the LBO pin goes low to indicate a low battery input voltage. The threshold has been set to 3.3V. The suggested value for R_{15} is 390k Ω . The value of R_{16} has been evaluated following the relation on the datasheet:

$$R_{16} = R_{15} \left(\frac{V_{bat}}{0.5V} - 1 \right) \simeq 2.2M\Omega \quad (4.18)$$

The inductor has been chosen to stand the switching current of the regulator and to have a low current ripple on the inductor. From the datasheet, the maximum average value of the current on the inductor is:

$$I_L = I_{out} \frac{V_{out}}{0.8V_{bat}} \quad (4.19)$$

Assuming $I_{out_{max}} = 2A$, in the worst case scenario $I_L = 3.8A$. Allowing $\Delta i_L = 0.1I_L$, the minimum inductance value is

$$L_{min} = \frac{V_{bat}(V_{out} - V_{bat})}{\Delta i_L f V_{out}} = 9.35\mu H \quad (4.20)$$

In which $f = 600kHz$ is the typical value of the switching frequency. Given this requirement a $10\mu H, 3.9A$ inductor has been chosen. The buck converter is the Texas Instruments TPS63050. This is actually a buck-boost, but in this project will be used just as a buck. It outputs a programmable voltage from $2.5V$ to $5.5V$ and a current of $0.5A$ with an efficiency around 90% [19]. The schematic of the circuit is shown in figure 4.19. All the components have been chosen following the

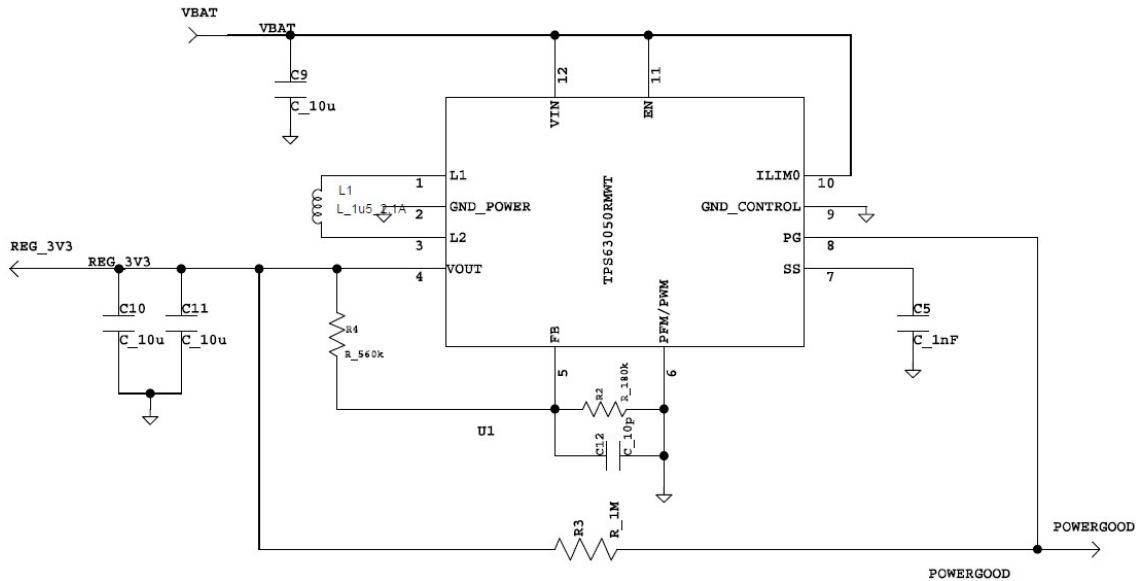


Figure 4.19: Schematic of TPS63050

suggestions on the datasheet. In particular, the resistances R_2 and R_4 were set to

give $V_{out} = 3.3V$; the suggested value for R_2 is $180k\Omega$ while R_4 has been evaluated as

$$R_4 = R_2 \left(\frac{V_{out}}{V_{FB}} - 1 \right) \simeq 560k\Omega \quad (4.21)$$

In which $V_{FB} = 0.8V$ is the voltage across R_2 . The powergood pin is used to check the output quality: this pin goes active low when the output voltage goes lower than 90% of the designed value.

4.5 Final layout

The circuit has been designed using the Mentor tool Expedition PCB. The PCB has been designed as a shield for the Arch Max board and has two layers, of which one is the ground plane, and the other one is for signals; however, some traces were routed on the ground plane too, when needed. For this prototype the receiving and transmitting antennas are different, but in future works a single antenna will be used. The receiver and the transmitter are well separated on the PCB, in order to not let the switching power amplifier affect the LNA. Also, the switching regulators have been separated, thus creating a zone in which just 5V traces are routed and one in which just 3.3V traces are routed. The ground is totally connected, avoiding the separation between the two zones not to create slots in the plane. Aside from the circuits described in the previous sections, some more components were added: a wet contact to detect when the system is in water (in figure 4.20 the schematic of the circuit) and a pressure sensor. The layout of the final system is shown in figure 4.21.

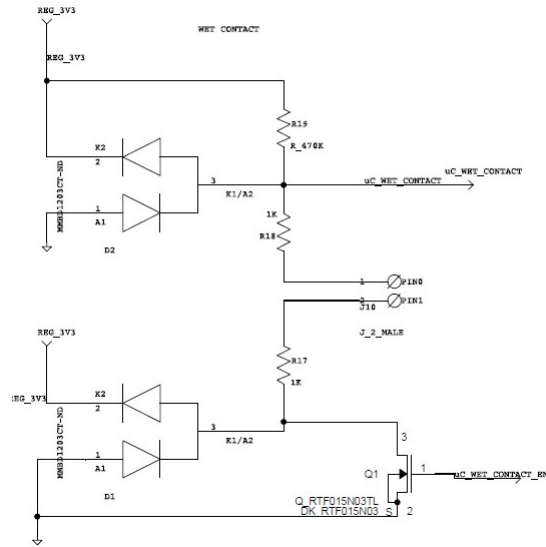


Figure 4.20: Circuit for wet contact

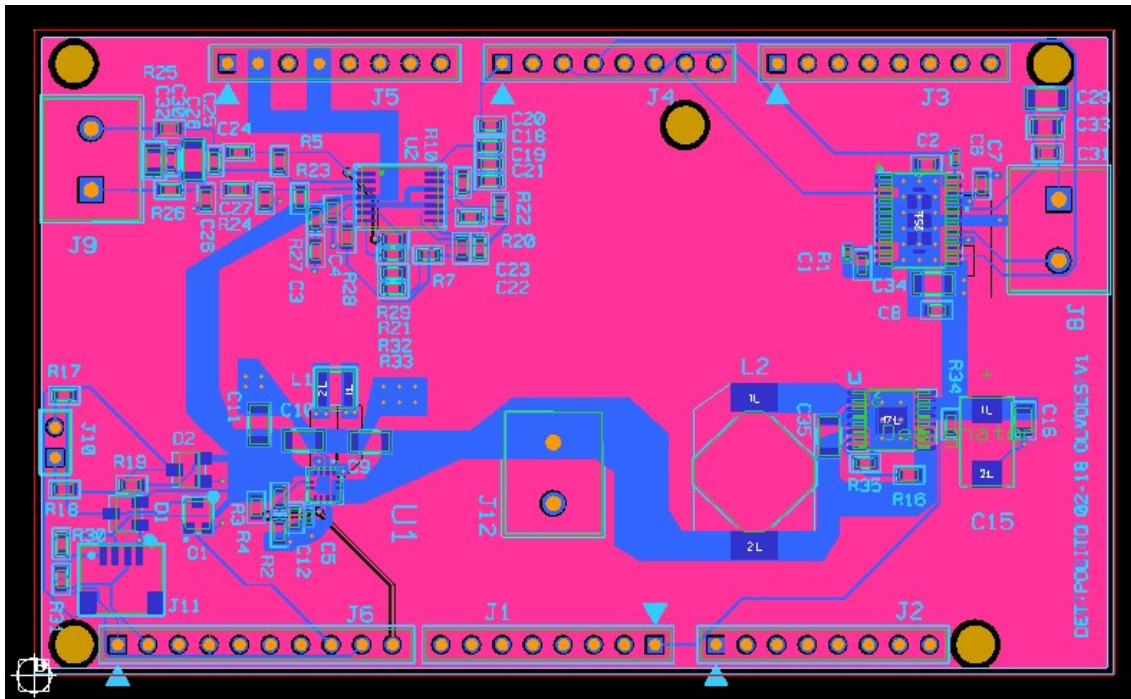


Figure 4.21: Layout of the system

Chapter 5

System testing

In this chapter the results of the testing of the developed system will be presented. With respect to the designed circuit, slightly lower resonating capacitances were used, thus leading to a higher resonating frequency $f_{res} = 11.2kHz$. Being the filter designed for a $10kHz$ resonance frequency, the receiver gain will be lower than the designed one. Due to lack of time and instrumentation, underwater measurements were not taken. So, the system has been tested in free air to check the transmitter and receiver behaviour.

5.1 Measurements on transmitter

The first measures were taken on the transmitting antenna. A stabilized DC power supply was used to generate an input supply voltage $V_s = 3.3V$. As an input signal, a $11.2kHz$ sine wave was generated with a waveform generator. The power amplifier was enabled pulling up the shutdown pin; the volume pin voltage was set to $3.3V$, thus giving a gain of $14dB$ (around 5 times). The amplitude of the input wave was increased until the saturation was reached. This happened for an input signal $V_{in} = 1.7V$. The measures were taken differentially with an oscilloscope. The results of the measurements are shown in figures 5.1, 5.2 and 5.3. In particular, in figure 5.1 you can see the voltage measured on the positive and negative terminal of the antenna; in figure 5.2 you can see a detail of the wave in which the switching due to the class D amplifier is shown; in figure 5.3 instead you can see the differential voltage at the antenna terminals. The average peak to peak voltage measured is around $130V$.



Figure 5.1: Positive and negative terminals of the transmitting antenna

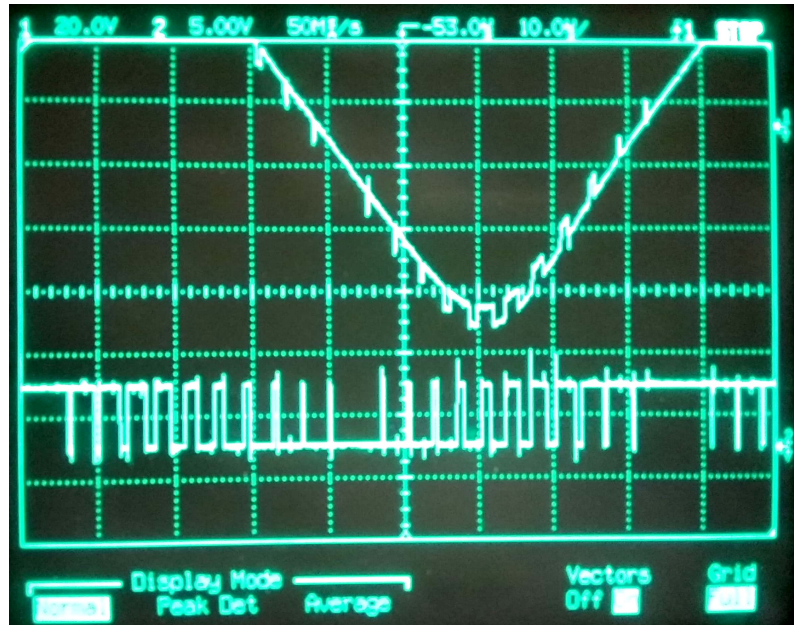


Figure 5.2: Detail of the wave showing the switching due to the class D amplifier

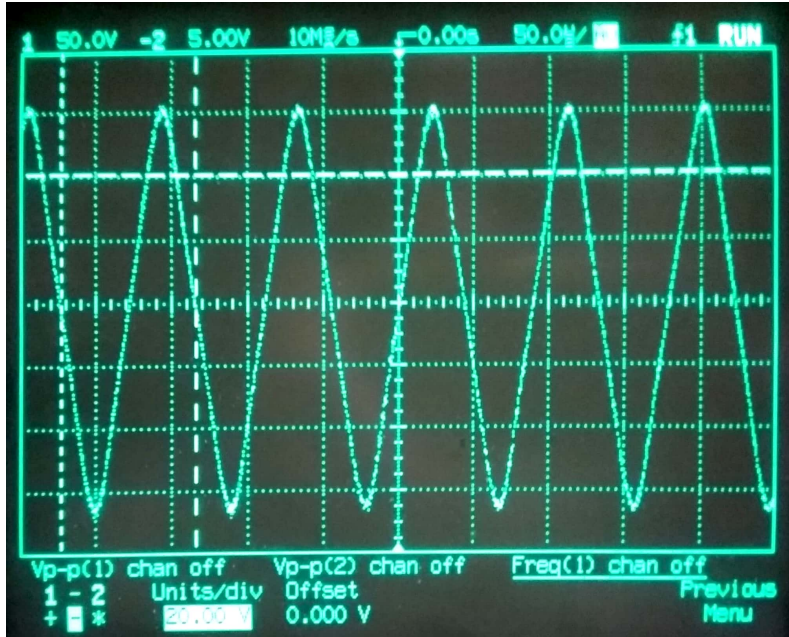


Figure 5.3: Differential output at the antenna terminals

This means that the maximum current flowing in the antenna will be:

$$I_{ppmax} = \frac{V_{ppmax}}{\sqrt{(\omega_r L_a)^2 + R_a^2}} = 0.202A \quad (5.1)$$

Finally, transmission with different frequencies was tried. Because of the LC resonator, transmission at frequencies much higher or lower than the resonating frequency is not as effective as the one at resonance frequency. This is shown in figures 5.4 and 5.5. In the first case a sine wave is still recognizable, even if the amplitude is much lower than the one at resonance. In the second case only the switching output of the class D amplifier is measured.



Figure 5.4: Voltage across the antenna terminals when a 1kHz signal is applied

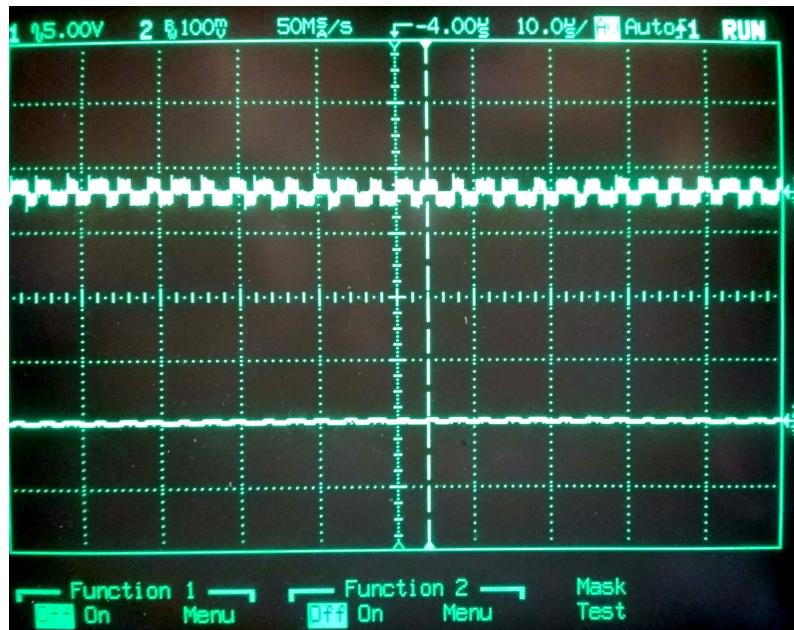


Figure 5.5: Voltage across the antenna terminals when a 100kHz signal is applied

5.2 Measurements on receiver

To test the receiver a waveform generator was used. A stabilized DC power supply was used to generate an input supply voltage $V_s = 3.3V$. First, a $11.2kHz$ waveform with a peak to peak voltage of $2mV$ was generated. The sine wave was given as an input to the receiver, not using the antenna. The output voltage from the filter was measured with an oscilloscope. The measured DC voltage was $V_{DC} = 1.62V$; the peak to peak amplitude of the output waveform was measured AC coupling the oscilloscope channel. The result of the measurement is shown in figure 5.6. The peak to peak amplitude of the wave is $V_{pp} = 750mV$; the gain is thus:

$$G = \frac{V_{ppout}}{V_{ppin}} = 375 \rightarrow 51.5dB \quad (5.2)$$

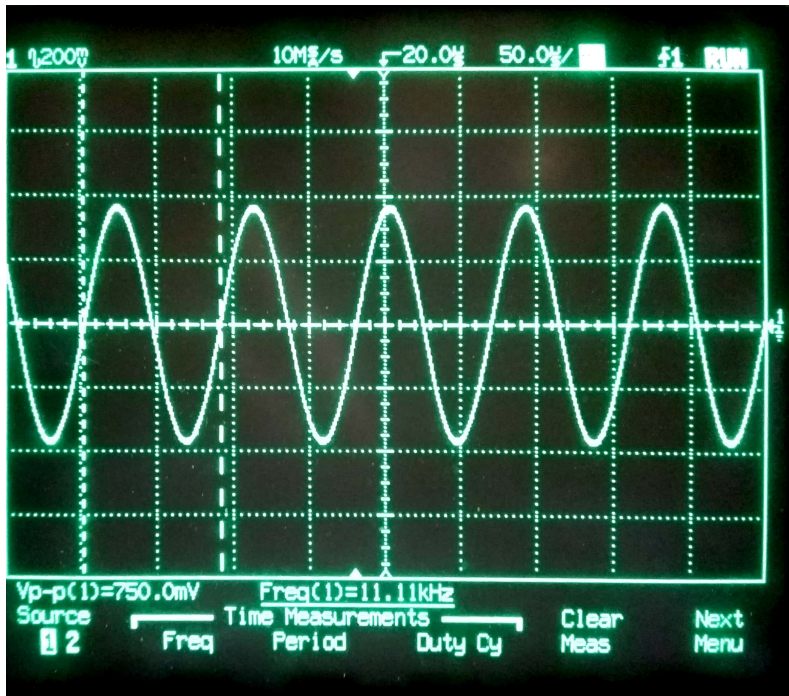


Figure 5.6: Receiver output signal

Then, the signal amplitude was increased until the saturation was reached. This happened for a peak to peak amplitude of the input waveform of $9.1mV$. The result is shown in figure 5.7; the maximum peak to peak amplitude achievable without

saturation is $V_{pp_{max}} = 3.47V$.

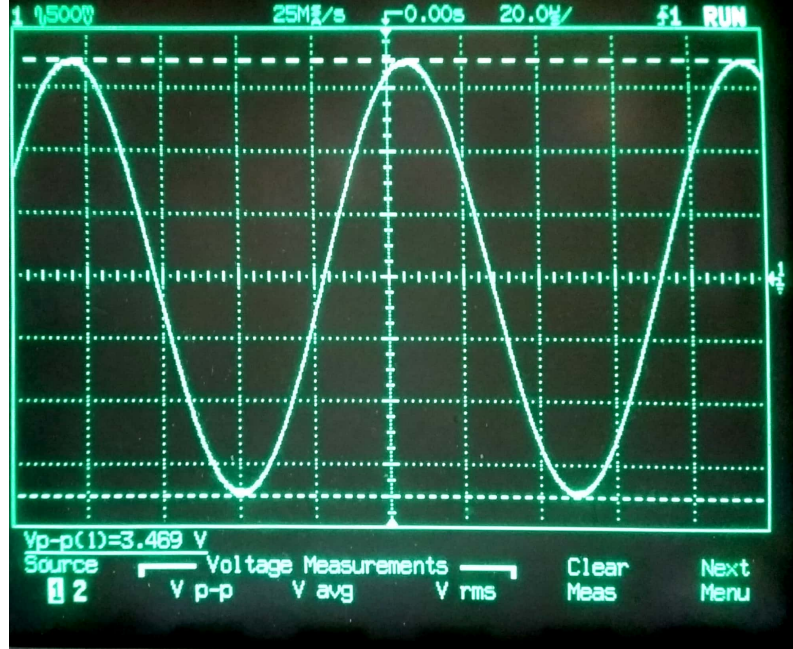


Figure 5.7: Maximum amplitude of the receiver output signal

Keeping the same input amplitude, a measure of the $-3dB$ bandwidth was made. The frequencies $f_{-3dB_{lo}}$ and $f_{-3dB_{hi}}$ are the one for which the output voltage is equal to:

$$V_{-3dB} = \frac{V_{pp_{max}}}{\sqrt{2}} = 2.44V \quad (5.3)$$

The results are shown in figures 5.8 and 5.9 and frequencies obtained are $f_{-3dB_{hi}} = 13.51kHz$ and $f_{-3dB_{lo}} = 8.36kHz$

Then, the gain one decade before and one decade after the nominal central frequency was measured. Hence, the frequency of the input waveform was set first at $1kHz$, then at $100kHz$; the input amplitude chosen was $V_{in} = 100mV$. The results of these measurements are shown in figures 5.10 and 5.11. At $1kHz$ the measured gain is:

$$G_{1kHz} = \frac{V_{pp_{1kHz}}}{V_{in}} = 0.58 \rightarrow -4.7dB \quad (5.4)$$

While at $100kHz$:

$$G_{100kHz} = \frac{V_{pp_{100kHz}}}{V_{in}} = 0.42 \rightarrow -7.5dB \quad (5.5)$$

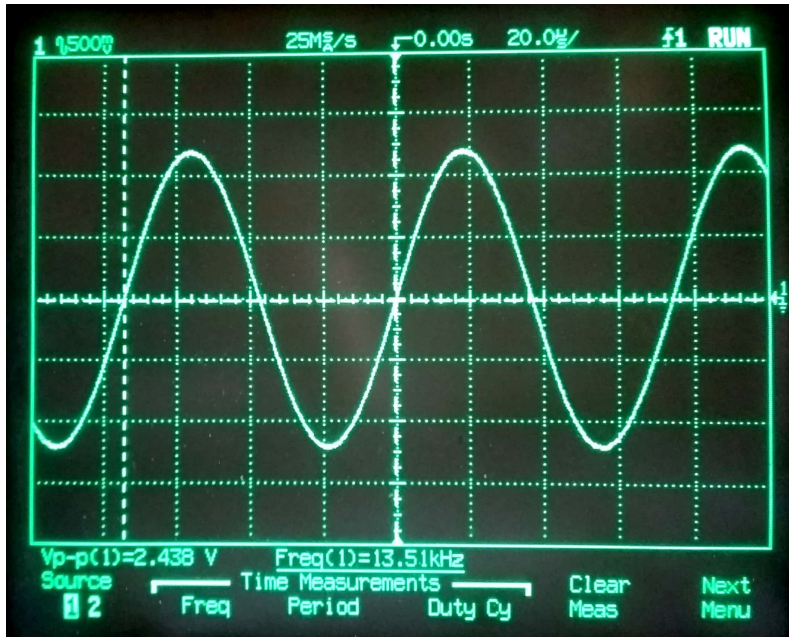


Figure 5.8: Measure of $f_{-3dB_{hi}}$

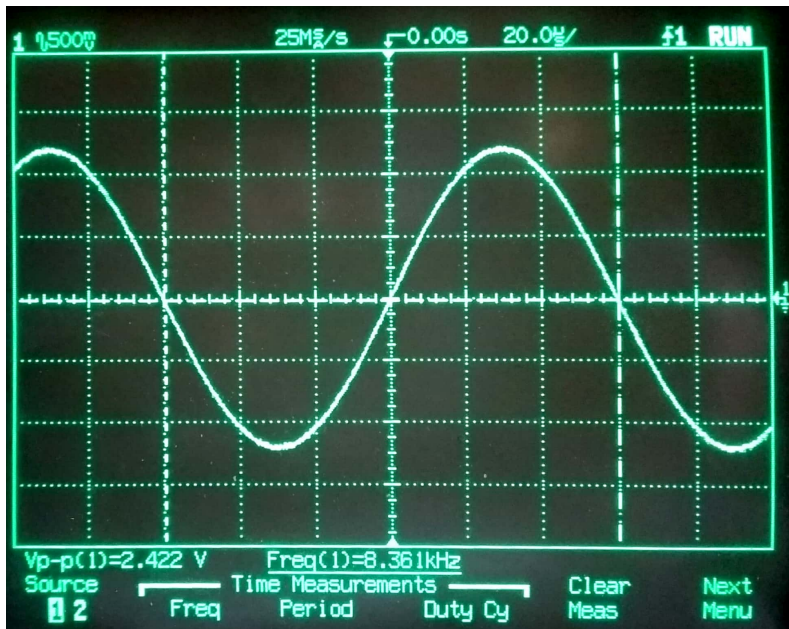


Figure 5.9: Measure of $f_{-3dB_{lo}}$

This means that the rising and falling slope in the receiver transfer function is approximately $-60\text{dB}/\text{dec}$ as designed.

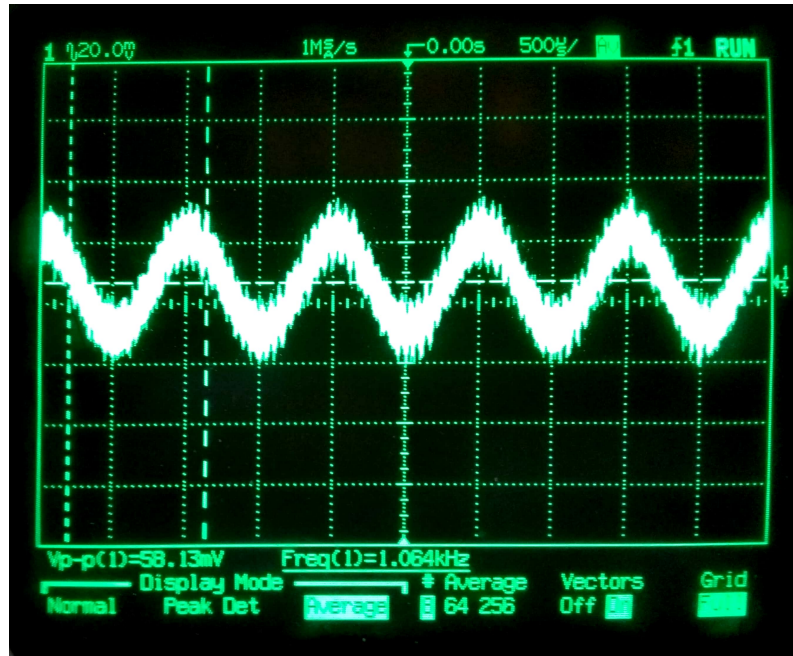


Figure 5.10: Gain measure at $f = 1\text{kHz}$



Figure 5.11: Gain measure at $f = 100\text{kHz}$

Finally, the amplitude of the input waveform was reduced to check the minimum

measurable input signal. Since the waveform generator minimum peak to peak voltage is $2mV$, a resistor divider was used to obtain lower amplitudes; an operational amplifier in voltage follower configuration was put between the input and the waveform generator output. Setting the resistor divider ratio to $4 * 10^{-3}$, the minimum peak to peak amplitude for which a good waveform was still measurable without distortions at the receiver output was $V_{in} = 12mV$, which means $V_{in_r} = 48\mu V$. The measured output voltage was $V_{out_{pp}} = 19.4mV$. This value is much higher than the one derived in section 4.3; considering the noisy environment in which the measures were taken, the lower bound if the input range is probably much lower than the measured one. The measured waveform is shown in figure 5.12.

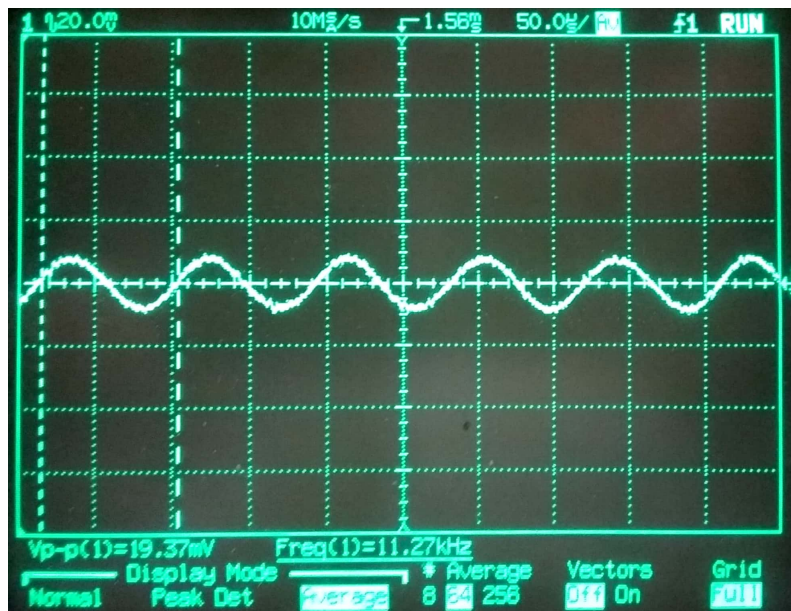


Figure 5.12: Output waveform for $V_{in_r} = 48\mu V$

5.3 Measurements with the antennas

Some measurements of the communication between the two antennas were tried. The measurements were taken in noisy and closed environments, which means that a lot of reflections were happening and that, for long distances, the signal to noise ratio was so low that it was impossible to understand which was the transmitted

signal and which the noise. Therefore, only some qualitative measures on the short range transmission and of the maximum distance for which a good signal to noise ratio is achievable were taken. The short range measures were taken using a normal oscilloscope while for long distances the USB oscilloscope Analog Discovery 2 was used. The antennas were put orthogonally to the floor and aligned. The transmitting antenna was fed by an input signal with a peak to peak amplitude of $130V$, corresponding to a generated input signal with a frequency of $11.2kHz$ and a peak to peak amplitude of $1.7V$. The minimum distance for which the receiver was not saturating is $d = 2.5m$ (figure 5.13). Then, to check the behaviour of the transmitted wave, measures at $d = 3m$ and $d = 3.5m$ were taken (figures 5.14 and 5.15).

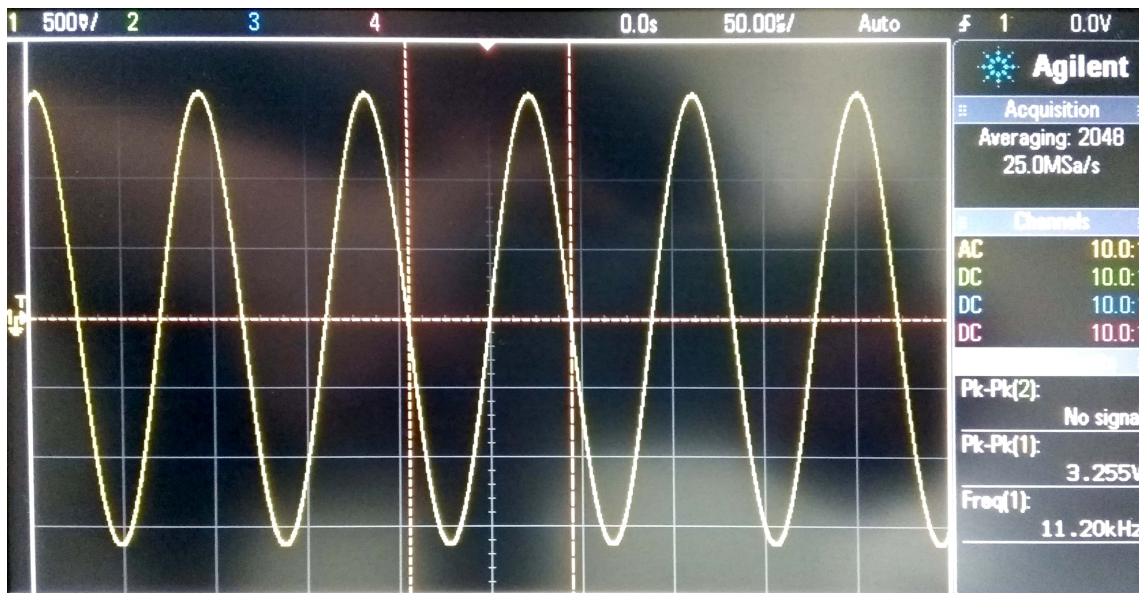


Figure 5.13: Receiver output voltage at $d = 2.5m$



Figure 5.14: Receiver output voltage at $d = 3m$



Figure 5.15: Receiver output voltage at $d = 3.5m$

Then, measures at longer ranges were taken. The first measure was taken at a distance $d = 10m$; the result of this measurement is shown in figure 5.16; as you

can notice, the environment is very noisy; it was possible to see a good sine wave averaging on 50 samples. The average peak to peak voltage measured is $152mV$.

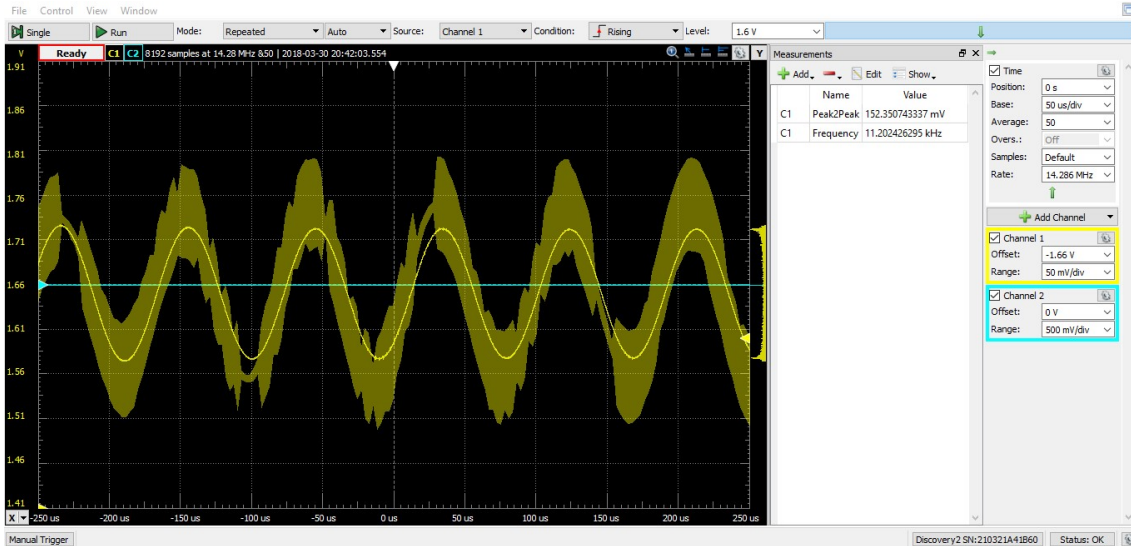


Figure 5.16: Receiver output voltage at $d = 10m$

Then, the antenna was brought to a distance $d = 15m$ from the transmitter. The measure taken is shown in figure 5.17. The measured peak to peak amplitude is $32mV$, but the measure is not so reliable due to the noise. A measure with a twenty meters distance between the antennas was tried; in this case the antenna was receiving mostly noise; in fact, switching off the transmitter didn't produce any significant change in the received signal. Thus, the maximum measured distance for which the antennas were still communicating is fifteen meters. In an open, less noisy environment, better quality measures could be taken and a larger distance could be probably achieved. Due to lack of time, it was not possible to take these measurements.

5 – System testing

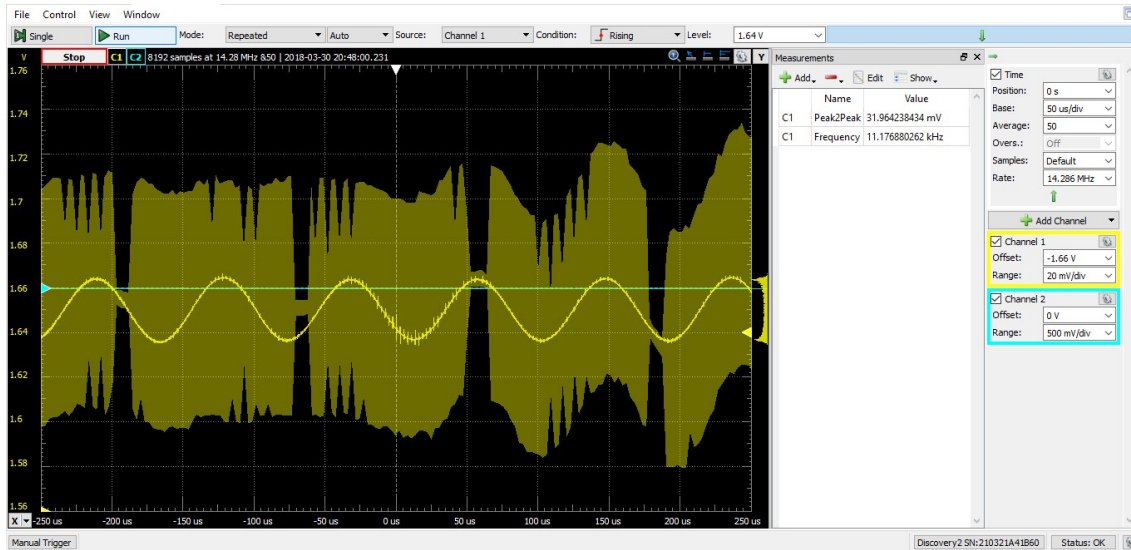


Figure 5.17: Receiver output voltage at $d = 15m$

Chapter 6

Conclusions and future work

The objective of this thesis was the development of a system for the transmission and reception of electromagnetic waves at very low frequencies. This project is in the framework of a bigger one, which aims at the development of a complete system for underwater communication between divers and between diver and stations on the surface. Due to lack of time, the system was not tested in underwater environment; besides, the transmission and reception has not been optimized because an antenna was not designed to be optimized with the system, but an already available one was chosen, with a large loss resistance that limits the current on the antenna and, therefore, the transmitted power and electromagnetic field. However, the transmitter and the receiver have been proven to be suitable for the transmission and reception: the former allows to generate low distortion, high amplitude sine waves; starting from the signal generator developed in [14], amplitudes in the order of hundreds of volts could be reached, leading to a $0.2A$ current with the antenna available in this project; using a higher Q , lower parasitic resistance antenna would lead to higher power, thus enhancing the transmission. The latter has been tested in a noisy environment proving that voltages around tens of microvolts in the frequency band could be sensed and correctly amplified, while the frequencies out of band are strongly attenuated thanks to the filtering stages and to the input LC resonating tank. Further developments could be made: for a future prototype, the transmission protocol could be addressed; besides, the final system will implement just one antenna for transmission and reception. If a half-duplex transmission is addressed, then the antenna could be connected to the circuit by means of a double-pole, double-throw switch; care should be applied, because the receiving and transmitting path deal with very different power levels. For what concerns the transmitter, the efficiency of the transmission could be further improved by trying to incorporate the antenna in the circuit for the generation of the sine wave (for instance using

a Wien oscillator with the antenna as inductor in feedback), in order not to use a separate signal generator; as for the receiver, a transformer could be inserted to allow a better power transfer by coupling the antenna impedance with the receiver input impedance. Finally, a study on the dimensions of the final system should be carried on (above all on the minimum dimension required for the antenna), to verify whether the portability is achievable or not, and a test underwater should be made to check the maximum distance achievable.

Bibliography

- [1] O. Aboderin, L. M. Pessoa, H. M. Salgado, "*Performance Evaluation of Antennas for Underwater Applications*," Wireless Days 2017, p. 4, March 2017.
- [2] X. Che, I. Wells, G. Dickers, P. Kear, X. Gong, "*Re-evaluation of RF electromagnetic communication in underwater sensor networks*," IEEE Commun. Mag., vol. 48, no. 12, pp. 143-151, December 2010.
- [3] R. Dunbar, "*The performance of a magnetic loop transmitter receiver system submerged in the sea*," Radio Electron. Engineer, vol. 42, no. 10, pp. 457-463, Oct. 1972.
- [4] A. Mazzanti, P. Andreani, "*Class-C harmonic CMOS VCOS with a general result on phase noise*," IEEE J. Solid-State Circuits, vol. 43, no. 12, pp. 2716-2729, Dec. 2008.
- [5] D. H. Gadani, V. A. Rana, S. P. Bhatnagar, A. N. Prajapati, A. D. Vyas, "*Effect of salinity on the dielectric properties of water*," Indian J. Pure Appl. Phys. vol. 50, pp. 405-410, 2012.
- [6] A. G. Miquel, "*UWB antenna design for underwater communications*," Universitat Politecnica de Catalunya, May 2009.
- [7] M. Orefice, "*Radiating System Notes, part II*," Dipartimento di elettronica, Politecnico di Torino.
- [8] A. Massaccesi, "*Analysis and design of underwater antennas for diving applications*," Politecnico di Torino, 2015.
- [9] S. I. Inacio, M. R. Pereira, H. M. Santos, L. M. Pessoa, F. B. Teixeira, M. J. Lopes et al., "*Antenna design for underwater radio communications*," OCEAN, 2016.
- [10] <http://www.radio-electronics.com/info/antennas/dipole/short-dipole-antenna.php>
- [11] <http://www.eryptick.net/unisold/loop.html>
- [12] Y. Liao, T. H. Hubing, D. Su, "*Equivalent circuit for dipole antennas in a lossy medium*," IEEE Transactions on Antennas and Propagation, vol. 60, no. 8, pp. 3950-3953, 2012.

- [13] S. K. Harriman, E. W. Paschal, U. S. Inan, "*Magnetic sensor design for femto-tesla low-frequency signals*," IEEE Trans. Geosci. Remote Sens..
- [14] D. Rakov, "*Development of an underwater communication system for scuba divers*," Politecnico di Torino, December 2017.
- [15] Maxim Integrated, "*Class D Amplifiers: Fundamentals of Operation and Recent Developments*", November 2017.
- [16] Texas Instruments, "*3-W STEREO CLASS-D AUDIO POWER AMPLIFIER WITH DC VOLUME CONTROL*", TPA2008D2 datasheet, July 2003, revised May 2004.
- [17] Texas Instruments, "*TLVx376 Low Offset and Drift, Low-Noise, Precision Operational Amplifiers for Cost-Sensitive Systems*", TLVx376 datasheet, October 2016.
- [18] Texas Instruments, "*TPS6103x 96% Efficient Synchronous Boost Converter With 4A Switch*", TPS6103x datasheet, September 2002, revised March 2015.
- [19] Texas Instruments, "*TPS6305x Single Inductor Buck-Boost With 1-A Switches and Adjustable Soft Start*", TPS6305x datasheet, July 2013, revised July 2015.
- [20] John G.Proakis, "*Digital Communications*, McGraw Hill – Chapter 5, 4th edition